

GRAIN ORIENTATION, PALEOCURRENTS, AND  
RESERVOIR TRENDS

By

HOWARD RICHARD BURMAN, JR.

Bachelor of Science

Oklahoma State University

Stillwater, Oklahoma

1971

Submitted to the Faculty of the Graduate College  
of the Oklahoma State University  
in partial fulfillment of the requirements  
for the Degree of  
MASTER OF SCIENCE  
May, 1973

OCT 8 1973

GRAIN ORIENTATION, PALEOCURRENTS, AND  
RESERVOIR TRENDS

Thesis Approved:

*John W. Shelton*

Thesis Adviser

*Douglas C. Keet*

*Tommy B. Thompson*

*Alex R. Ross*

*N. A. Durbin*

Dean of the Graduate College

## PREFACE

This thesis is primarily a study of grain orientation as a paleocurrent indicator and as it relates to sand trends. Grain orientation, measured by bulk methods, is facilitated by the use of Shell Development Company's COBRA, a conductivity anisotropy instrument. These studies embrace a number of sand-depositing environments, involve three-dimensional grain orientation, and include in situ measurements of sand deposited by an active process.

The writer expresses his appreciation to individuals who provided assistance and guidance to him during the study. Dr. J. W. Shelton suggested the investigation and provided invaluable assistance, both in the field and during the writing of the paper. Thanks are extended to advisory committee members, Dr. D. C. Kent, who assisted the field party during the Cimarron River project, and Dr. T. B. Thompson, who assisted in the thin section study. A grateful thanks goes to Barbara Cunningham whose confidence, encouragement, and understanding hastened the completion of this study. The author wishes to thank Dixie Dobbs whose advice and proofreading ability were invaluable, and his parents, Mr. and Mrs. Howard R. Burman, and brothers, Roger and Jim, who provided a welcome retreat, moral support, and constant encouragement during his graduate studies. Ray Noble and Mike McGuire, fellow graduate students, provided much help of both a technical and nontechnical nature.

## TABLE OF CONTENTS

Chapter	Page
I. ABSTRACT . . . . .	1
II. INTRODUCTION . . . . .	3
Objectives . . . . .	4
Methods . . . . .	4
Previous Investigations . . . . .	5
III. GRAIN ORIENTATION IN BARRIER-BAR DEPOSITS . . . . .	9
Galveston Island . . . . .	9
Geologic Setting . . . . .	9
Grain Orientation and Imbrication . . . . .	10
Eagle Sandstone . . . . .	16
Stratigraphic Framework . . . . .	16
Depositional Environment and Trend . . . . .	18
Grain Orientation and Imbrication . . . . .	18
IV. GRAIN ORIENTATION IN SHALLOW MARINE-SHOREFACE DEPOSITS . . . . .	23
Harding Sandstone . . . . .	23
Stratigraphic Framework . . . . .	23
Depositional Environment and Trend . . . . .	24
Grain Orientation . . . . .	24
Burgen Sandstone . . . . .	28
Stratigraphic Framework . . . . .	28
Depositional Environment and Trend . . . . .	30
Grain Orientation . . . . .	30
Trinidad Sandstone . . . . .	35
Stratigraphic Framework . . . . .	35
Depositional Environment and Trend Indicators . . . . .	37
Grain Orientation . . . . .	38
V. GRAIN ORIENTATION IN DELTAIC DEPOSITS: VAMOOSA FORMATION . . . . .	42
Stratigraphic Framework . . . . .	42
Depositional Environment and Trend . . . . .	45
Grain Orientation . . . . .	45
Correlation of Grain Orientation and Paleocurrents . . . . .	52

Chapter	Page
V. (CONTINUED)	
Change in Grain Orientation With Time . . . . .	52
VI. GRAIN ORIENTATION IN A BRAIDED-MEANDERING STREAM: CIMARRON RIVER . . . . .	55
Geologic Setting . . . . .	55
Grain Orientation . . . . .	56
In Situ Measurements . . . . .	56
Laboratory Measurements . . . . .	56
VII. SUMMARY . . . . .	63
REFERENCES CITED . . . . .	65
APPENDIX A - COBRA MEASUREMENT . . . . .	69
APPENDIX B - IN SITU MEASUREMENT . . . . .	73
APPENDIX C - IMPREGNATION TECHNIQUES . . . . .	76
APPENDIX D - COMPUTER PROGRAM: CHAYES' MINIMUM VARIANCE FABRIC MEAN . . . . .	79
APPENDIX E - RATING OF QUALITY OF RESULTS . . . . .	83

LIST OF TABLES

Table	Page
I. Grain Imbrication in Galveston Island Sand . . . . .	13
II. Grain Imbrication in Lowermost Unit Eagle Sandstone . . . . .	22
III. Grain Orientation in Harding Sandstone . . . . .	26
IV. Grain Orientation in Burgen Sandstone . . . . .	32
V. Grain Orientation in Trinidad Sandstone . . . . .	38
VI. Grain Imbrication in the Trinidad Sandstone . . . . .	40
VII. Grain Orientation in the Vamoosa Formation . . . . .	48
VIII. Comparison of Grain Orientation Measurements to Other Current Indicators . . . . .	60

LIST OF FIGURES

Figure	Page
1. Location map of Galveston Island, Texas, and environs . . . . .	11
2. Galveston Island Sand imbrication . . . . .	12
3. Imbrication in Galveston Island Sand (sample 69A) . . . . .	14
4. Imbrication in Galveston Island Sand (sample 69B) . . . . .	15
5. Isopach map of lowermost sandstone unit of the Eagle Sandstone . . . . .	17
6. Imbrication in the lowermost unit of the Eagle Sandstone . . . . .	19
7. Imbrication in Eagle Sandstone (sample 106) . . . . .	20
8. Imbrication in Eagle Sandstone (sample 97) . . . . .	21
9. Lithofacies and isopach map of the Harding Sandstone . . . . .	25
10. Grain orientation in Harding Sandstone . . . . .	27
11. Grain imbrication in Harding Sandstone . . . . .	29
12. Location map showing distribution of Burgen Sandstone . . . . .	31
13. Grain orientation in Burgen Sandstone . . . . .	33
14. Grain imbrication in Burgen Sandstone . . . . .	34
15. Regional trend(s) of Trinidad Sandstone . . . . .	36
16. Grain orientation in Trinidad Sandstone . . . . .	39
17. Grain imbrication in Trinidad Sandstone . . . . .	41
18. Sand distribution map of Vamoosa Formation . . . . .	43
19. Grain orientation in the lower unit of Vamoosa Formation . . . . .	46
20. Grain orientation in the lower middle unit of Vamoosa Formation . . . . .	47

Figure	Page
21. Grain orientation in the upper middle unit of Vamoosa Formation . . . . .	49
22. Grain orientation in the upper unit of the Vamoosa Formation . . . . .	50
23. Composite grain orientation in the Vamoosa Formation . . . . .	51
24. Paleocurrent indicators and grain orientation in Elgin Sandstone . . . . .	53
25. Change in paleocurrent direction with time . . . . .	54
26. Map of Cimarron River, showing medium-scale cross-bedding direction . . . . .	57
27. Map of Cimarron River, showing current trends from parting lineation . . . . .	58
28. Directional features in Cimarron River sand deposits . . . . .	59
29. Grain orientation in medium-scale cross-bedding . . . . .	61
30. Grain orientation in horizontal bedding . . . . .	62



## CHAPTER I

### ABSTRACT

Grain orientation has proved to be an accurate paleocurrent indicator. With bulk methods, such as those performed with the conductivity anisotropy instrument, COBRA, measurements can be made rapidly and accurately for a vast number of sand grains.

Grain orientation has been examined in various sand-depositing environments. In the case of strandline (barrier-bar) and certain shallow marine environments, grain orientation is found to be approximately normal to sandstone-body trend. In this study, these environments are represented by the Recent Galveston Island barrier sand, the Cretaceous Eagle Sandstone, the Ordovician Harding Sandstone, the Ordovician Burgen Sandstone, and the Cretaceous Trinidad Sandstone. Imbrication in all these units except the Harding show a shoreward dip and thereby indicate deposition is dominantly by backwash. The Harding is believed to be the product of a stable shelf environment, with imbrication resulting from shoreward-directed currents.

Deltaic environments are represented by the Pennsylvanian Vamoosa Formation, in which grain orientation shows favorable results compared to megascopic paleocurrents. The Vamoosa is divided into four subdivisions, and the average grain orientation, from older to younger units, shows a rather progressive westerly change in direction. This relationship suggests change in source areas with time.

The Cimarron River study was undertaken to prove the adaptability of the COBRA for field measurements utilizing an in situ probe. Grain orientation measurements correlated well with the paleocurrent measurements. All indicators show a direction parallel with the trend of the sand body.

In this study, new techniques and improvements have been made in impregnation methods and COBRA measurements, both laboratory and in situ. These improvements result in better consolidated cores and more rapid and reliable sample measurement.

## CHAPTER II

### INTRODUCTION

Although grain orientation has been considered by various workers as a valid paleocurrent indicator in horizontally bedded sands and sandstones, the slow cumbersome optical methods used in the past have prevented it from becoming widely used. In relatively recent years, several bulk methods have been developed to measure grain orientation rapidly. One of these methods utilizes an instrument that measures conductivity anisotropy in a cylindrical plug drilled from a sample. This instrument has proved to be very accurate and extremely rapid. For example, the grains measured in this study number approximately  $1.5 \times 10^9$  and required about 240 man-hours to measure. On the other hand, some 2000 grains, measured visually from thin sections, required about 40 man-hours of measurement. The grains analyzed in this study by bulk methods would require approximately 15,000 man-years for visual analysis. It is estimated that laboratory measurements, by conductivity anisotropy, are  $10^4$  to  $10^5$  times faster than optical methods. The conductivity anisotropy instrument is equipped with an in-situ probe for field use in unconsolidated sediments. This method is approximately 5 times faster than the standard laboratory method.

## Objectives

The primary objective of this study is to relate grain orientation, measured by means of Shell Development Company's conductivity anisotropy instrument, (COBRA), to paleocurrent (or current) directions and sand trend. Evaluation of grain orientation has been made by study of it in a number of sands and sandstones representing several depositional environments. Three-dimensional analysis has been made of grain orientation in a number of these deposits.

Another objective of this study is to relate grain orientation to active depositional agents, such as the Cimarron River in central Oklahoma and shoreline processes at Galveston Island, along the Texas Gulf Coast.

The results of this study are given according to the sand-depositing environment. The sands and sandstones are grouped for discussion into strandline (barrier-bar), shallow marine-shoreface, deltaic, and alluvial deposits.

## Methods

Grain orientation was determined in this study by the use of COBRA, an instrument measuring grain orientation by conductivity anisotropy. Oriented cylinders  $7/8$  in. long and  $3/4$  in. in diameter are rotated between the plates of a capacitor. A maximum deflection, indicated by an ohm-meter, reflects an anisotropic fabric. The preferred grain orientation corresponds to this maximum deflection, which is related directionally to the reference mark denoting plug

orientation. Five plugs are preferred for analysis, but a minimum of 3 is acceptable.

COBRA analysis was made of grain orientation in 80 samples -- 47 laboratory and 33 in situ measurements. Details of this procedure are discussed in Appendices A and B. Results are included from 84 samples measured by various workers using both the COBRA and Dielectric Anisotropy (DA) instruments. Eleven samples of unconsolidated sand were collected and impregnated with an epoxy cement to prepare them for measurement by standard laboratory procedures (Appendix C). Four thin sections were analyzed visually by means of photomicrographs, and the data were processed by a computer program designed to compute Chayes' minimum variance fabric mean and standard deviation (Appendix D). Preferred grain orientation directions were plotted on azimuth diagrams, from which trends of sediment transport were estimated. A 30°-sliding average was utilized in preparing many of the diagrams. In this procedure raw data are divided into 10° classes, and the total value recorded for each class represents the numbers (of readings or measurements) in that class plus the numbers for each of the adjoining 10° classes.

#### Previous Investigations

Grain orientation has been compared to other paleocurrent indicators such as cross-bedding, flute casts, groove casts, parting lineation, rib-and-furrow structure, and sole marks. Overall, it is determined to be a valid paleocurrent indicator by the majority of workers, such as Nanz (1960), McBride (1962), Pettijohn (1962), McBride

and Yeakel (1963), Potter and Mast (1963), Spotts (1963), Dodge (1968), and Shelton and Mack (1970).

Basically, two methods have been used by the many workers who have measured grain orientation. Individual grains are measured visually, in thin sections or photomicrographs, in the particulate method. This has proved to be an arduous task even though a statistically small number of grains is measured. Overall, the method shows good quality of results, however.

In more recent years, several developments have been made that permit grain orientation to be measured by a bulk method, involving a phenomenally large amount of grains. These methods are based on physically derived properties resulting from preferentially oriented grains. Diverse bulk methods have been utilized by workers such as Martinez (1958), Pierson (1959), Arbogast, et al. (1960), Nanz (1960), Zimmerle and Bonham (1962), Mast and Potter (1963), Orr (1964), Pincus and Dobrin (1966), Rodriguez and Pirson (1968), Rees (1971), and Winkelmoelen (1972).

Photometer methods were developed and used by Martinez (1958) and Pierson (1959). The basic premise of this method is that a consistent relationship exists between grain morphology and optic-axis orientation. Zimmerle and Bonham (1962) used a method involving a flying-spot scanner, in which a beam of light scans a photomicrograph transparency. A photoelectric cell records the number of times a grain is encountered by the scanning beam. Scans parallel to elongate axes thus measure fewer encounters than scans perpendicular to long axes.

The dielectric anisotropy (DA) method, described by Nanz (1960) and Arbogast, et al. (1960) and used by Matalucci, et al. (1969) and

Shelton and Mack (1970), is based on the concept that the direction of maximum dielectric coefficient is equivalent to average grain orientation.

Rodriguez and Pirson (1968) have hypothesized that the focused and oriented resistivity or conductivity values, measured during a dipmeter survey, can be correlated with dominant grain orientation. Pincus and Dobrin (1966) experimented with a method wherein a laser beam is transmitted through a photomicrograph transparency. The diffraction pattern yields information of the statistical distribution of direction and spatial frequencies associated with all elements of the photograph.

The method used in this study is the conductivity anisotropy (COBRA) technique described by Orr (1964) and used by Terrell (1972). It is very similar in principle to the dielectric anisotropy (DA) method described by Nanz (1960) and Arbogast, et al. (1960). Results from this method obtained by other workers were also used in this study.

Rees (1971) used a bulk method utilizing the magnetic susceptibility of magnetite in sandstone as a grain-orientation indicator. He suggests elongate magnetite grains are oriented parallel to current flow just as regular sand grains would be. This elongation created a minute magnetic anomaly concentrated parallel to this elongation. This anomaly is measured in a small plug with a sensitive magnetometer.

Winkelmolen (1972) believes that dielectric and conductivity anisotropy bulk methods do not measure grain orientation exclusively. He contends that cross-bedding, certain measuring principles of symmetry, and crystal-lattice orientation may cause anomalous readings.

He also experimented with procedures for improving bulk-measurement techniques. His criticisms were not recognized as pertinent to this study because measurements reported herein have been calibrated to other features and samples have been carefully selected.



## CHAPTER III

### GRAIN ORIENTATION IN BARRIER-BAR DEPOSITS

Galveston Island along the Gulf Coast of Texas and the Cretaceous Eagle Sandstone at Billings, Montana, are similar in depositional environment but differ in the direction of accretion with respect to the mainland and in size and space relationships.

#### Galveston Island

##### Geologic Setting

Galveston Island is 3 to 5 mi. wide, approximately 35 mi. long, and 40 ft. or less in sand thickness. It shows gradational lower and lateral boundaries.

Depositional features of the foreshore are horizontal lamination and very low-angle cross-bedding (Bernard, et al., 1962). The horizontal lamination conforms to the gentle slope of the beach, which averages less than  $5^{\circ}$ . These deposits are typically burrowed and mottled in the lower part. The sand is gray to brown, fine-grained, and very well sorted. There is an overall upward increase in grain size.

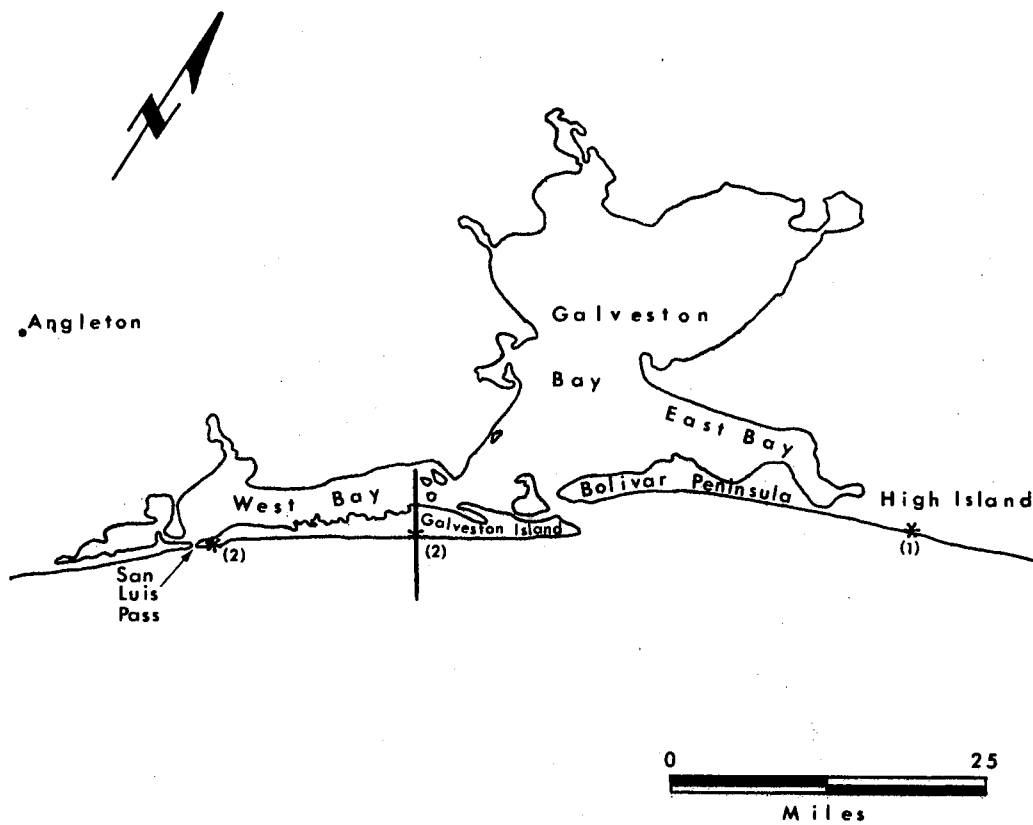
Galveston Island began as a small bar about 4 mi. offshore in 5 to 8 ft. of water. The island has grown seaward by beach accretion and southwestward, parallel to the shore, by spit accretion due to longshore drift. Growth on the backshore side by accretion is

of minimal importance (Bernard, et al., 1962). The source of the sand is mainly from an easterly source, such as Pleistocene and Recent Mississippi River sands being reworked and transported by longshore drift and sands from the Trinity and San Jacinto Rivers (Hsu, 1960).

#### Grain Orientation and Imbrication

Nanz (1955) and Curray (1956) have determined that grain orientation in the Gulf Coast beach environment, in the upper part of a barrier-bar sequence, is perpendicular to the shoreline trend.

For this study, 5 samples were analyzed by bulk methods (COBRA and DA) and 2 thin sections were analyzed. Four of the samples were collected from Galveston Island, and the other was collected from High Island to the east-northeast (Figure 1). All of the samples were collected on the foreshore or berm of the beach, several in. below the surface, in plastic or metal sleeves. After the samples were impregnated with an epoxy cement in the laboratory, plugs were drilled in the horizontal direction perpendicular to grain orientation for imbrication measurements. Imbrication was also studied in 2 thin sections of Galveston Island sand by means of photomicrographs. Results of all the measurements, tabulated in Table I and plotted in Figure 2, indicate that the more prominent grain imbrication is to the northwest at a gentle angle. Some COBRA measurements indicate imbrication to the southeast, but those results are generally regarded as less reliable. For example, only one plug was obtainable from one sample, and the high range of measurements in another sample suggests disturbance, due possibly to poor sample-processing technique or bioturbation.



- \*-Sample Location
- (2)-Number of Samples Per Location
- \-Grain Orientation

Figure 1. Location map of Galveston Island, Texas, and environs. Grain orientation is approximately normal to the sand trend (Curry, 1956).

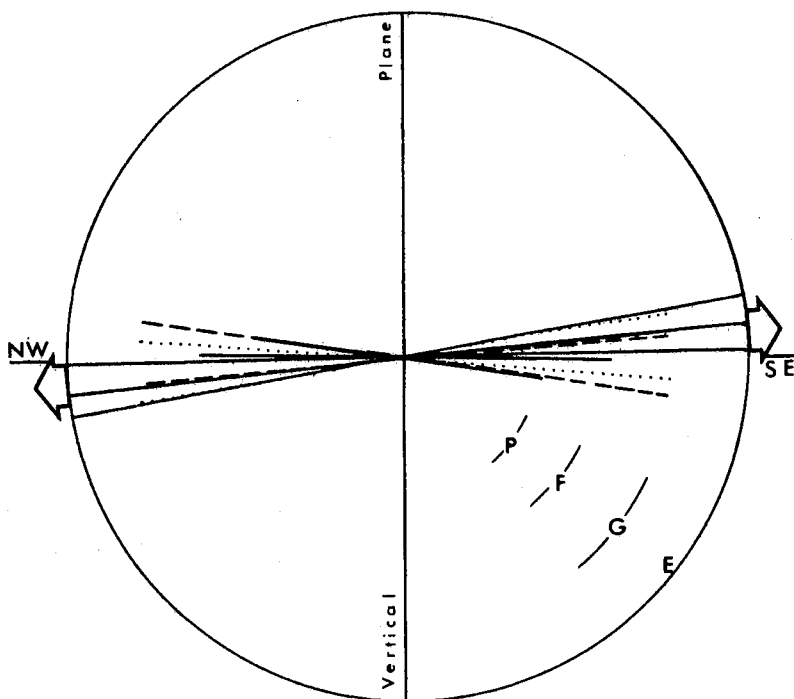


Figure 2. Diagram showing imbrication in Galveston Island Sand. Solid lines are results of COBRA measurements; dashed lines are results from thin sections; and dotted lines are DA measurements. Overall weighted average shows an imbrication of  $4^{\circ}$  to the northwest. Length of line corresponds to quality of results. E = Excellent, G = Good, F = Fair, and P = Poor.

TABLE I  
Grain Imbrication in Galveston Island Sand

Sample No.	No. Plugs	No. Grains	Range in Measurements	Results	Quality <sup>1</sup>
GIL	4	--	17°	10°NW	E
GIU	1	--	--	9°SE	P
SL-1	3	--	3°	6°NW	E
SL-2	4	--	66°	1°SE	F
HI	3	--	6°	1°NW	E
69A-TS <sup>2</sup>	-	485	--	6°NW	G
69B-TS <sup>2</sup>	-	511	--	8°SE	G
69A-DA <sup>3</sup>	2	--	10°	4°SE	G
69B-DA <sup>3</sup>	2	--	10°	10°NW	G

<sup>1</sup>See Appendix E for rating of quality of results. E = Excellent, G = Good, F = Fair, P = Poor.

<sup>2</sup>TS - Thin Section

<sup>3</sup>DA - Dielectric Anisotropy Measurement

Visual grain orientation data were obtained by measuring the apparent long axis in thin section. The data from this "long dimension method" were processed by a computer program (Appendix D), utilizing Chayes' minimum variance technique to determine a fabric mean. The average imbrication direction in one sample is northwest at 6° (Figure 3) and is southeast at 8° (Figure 4) in the other. The distributions with standard deviations of 41° and 44° indicate that the quality is good. However, imbrication measured by the DA

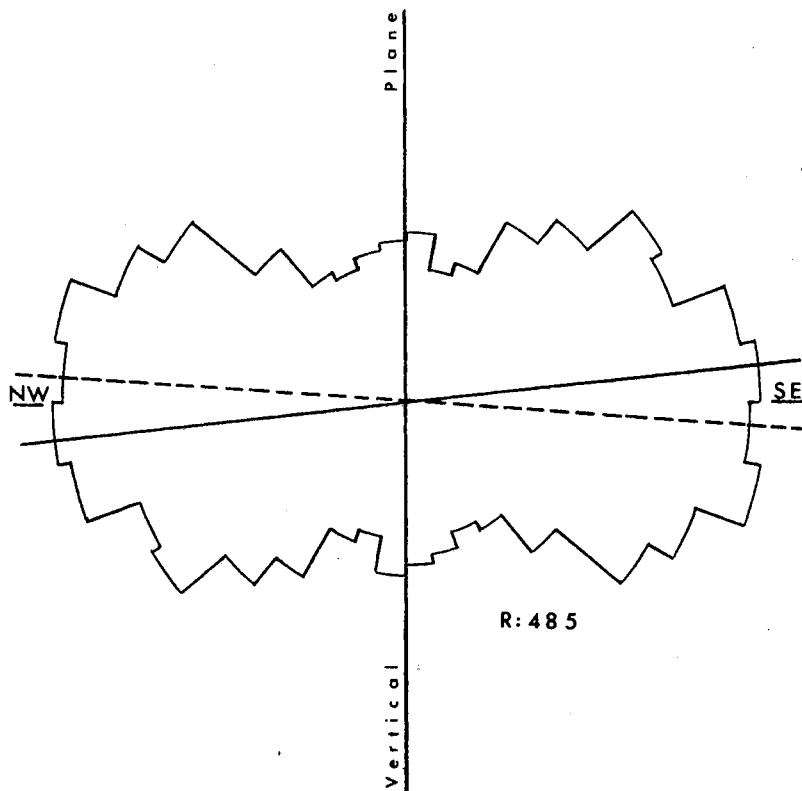


Figure 3. Grain imbrication in Galveston Island Sand (sample 69A). R = total number of grains measured. A 30°-sliding average was used in preparation of diagram. Solid line with dip to northwest at 6° is calculated preferred direction, using Chayes' minimum variance fabric mean. Dashed line is orientation by DA instrument, which shows dip to southeast at 4°.

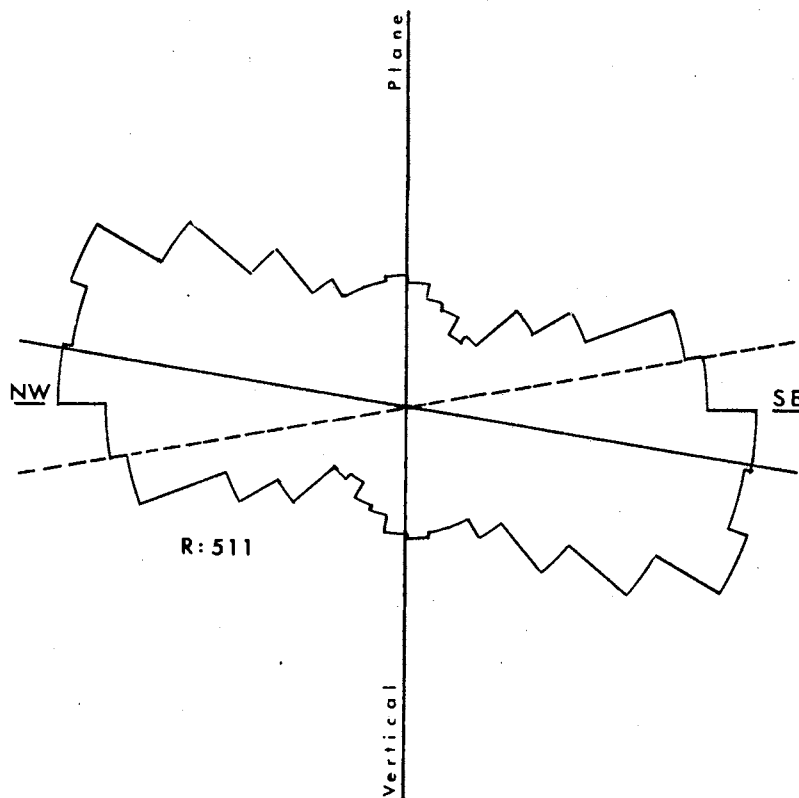


Figure 4. Grain imbrication in Galveston Island Sand (sample 69B).  $R$  = total number of grains measured. A  $30^\circ$ -sliding average was used in preparation of diagram. Solid line with dip to southeast at  $9^\circ$  is calculated preferred direction, using Chayes' minimum variance fabric mean. Dashed line is orientation by DA instrument, which shows dip to northwest at  $10^\circ$ .

Instrument for each sample is in an opposite direction to that determined visually. The low angle of imbrication suggests that both wash and backwash are operative in orienting sand grains. However, the more prominent northwesterly dip suggests that backwash is the more important process.

### Eagle Sandstone

#### Stratigraphic Framework

The lowermost unit of the Upper Cretaceous Eagle Sandstone is present in a linear band, which trends N25°W through Billings, Montana (Figure 5). The Eagle consists of as many as 5 sandstones, and the lowermost unit overlies the Telegraph Creek Formation, a sequence of shales and siltstones (Weimer, 1960).

The lowermost sandstone unit of the Eagle Sandstone reaches a maximum thickness of 100 ft. in the Billings area and thins east and west to 0. It varies in width from 20 to 30 mi. in the study area. The lower and lateral boundaries are gradational (Shelton, 1965). The upper boundary is thought to represent an erosional surface which formed during a minor transgression. Large-scale, low-angle inclined bedding, dipping S60°W, or almost normal to the sandstone trend, is the dominant structure of the upper part of the lowermost unit (Shelton, 1965). The sand is poorly sorted and is very fine- to fine-grained, with an upward increase in grain size. Common constituents besides quartz are chert and rock fragments (Shelton, 1965).



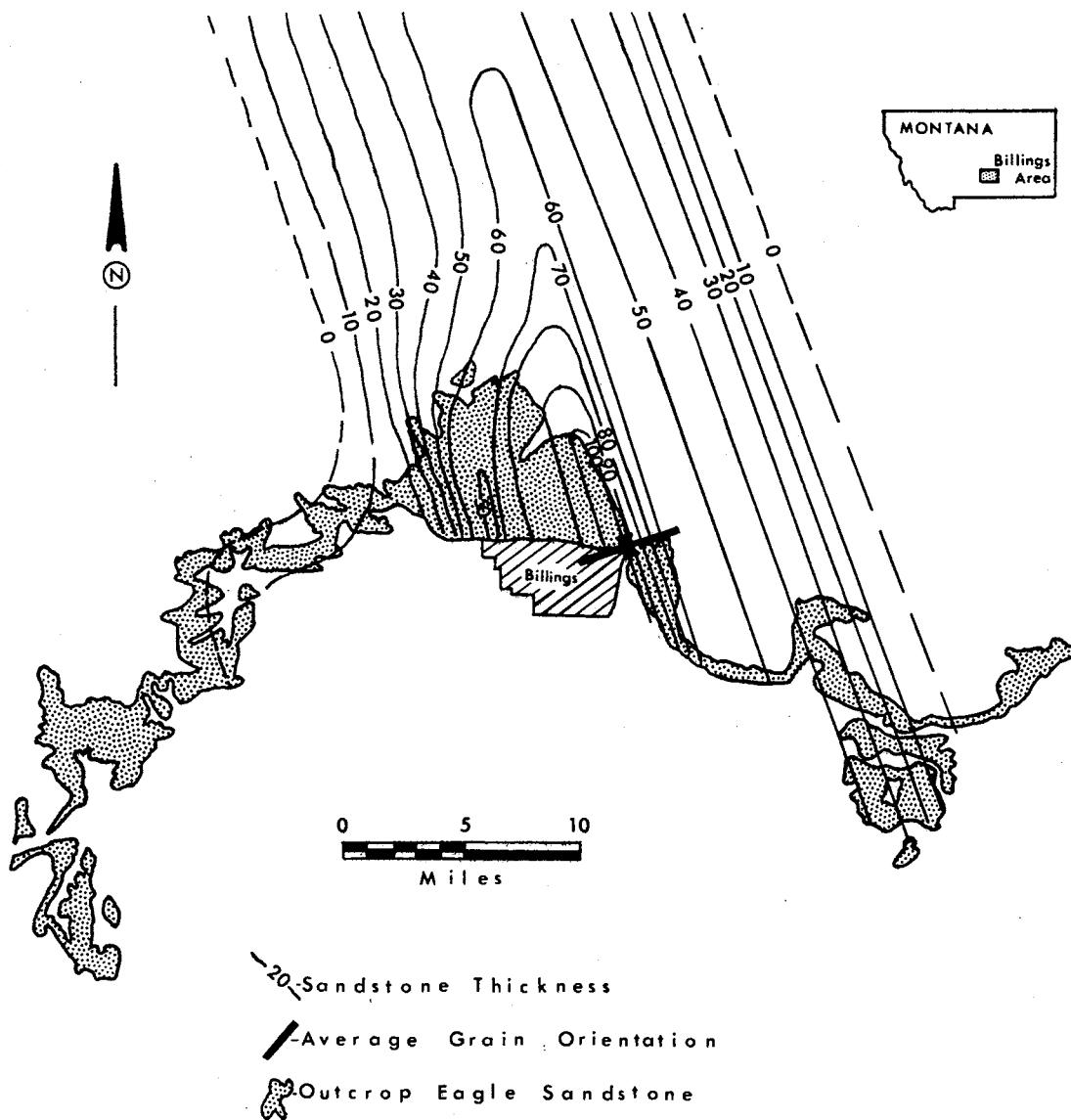


Figure 5. Isopach map of the lowermost sandstone unit of the Eagle Sandstone at Billings, Montana, showing a trend of  $N25^{\circ}W-S25^{\circ}E$ . Grain orientation is approximately normal to the trend.

### Depositional Environment and Trend

The lowermost unit began as a barrier-bar, probably more than 50 mi. offshore in water ranging 60 to 75 ft. in depth (Shelton, 1965). The bar paralleled the north-northwest paleogeographic strandline that existed in Late Cretaceous time (Weimer, 1960). Inclined beds and the lateral repetition of the vertical sequence indicate an offlap sequence, representing growth by westward accretion toward the mainland. Seaward growth, by accretion, is thought to have been minor because of the absence of east-dipping inclined beds (Shelton, 1965).

### Grain Orientation and Imbrication

Grain orientation in the lowermost unit is approximately perpendicular to the sandstone trend (Shelton and Mack, 1970). Bulk measurement of 2 samples and analysis of 2 thin sections were made to determine imbrication. Because grain orientation is perpendicular to the trend, the samples were drilled parallel to trend. Results show an average imbrication of  $7^\circ$  to the east (Figure 6; Table II). Two thin sections, with the same orientation as plugs for bulk method measurements, were analyzed visually for imbrication by means of photomicrographs. The data were processed by a computer program designed to compute Chayes' minimum variance fabric mean, which, for sample 106, is  $25^\circ\text{E}$  and  $15^\circ\text{W}$  for sample 97 (Figures 7 and 8). Standard deviation, calculated by the program as  $48.0^\circ$  and  $49.5^\circ$ , respectively, indicate results for both samples are fair in quality.

The data suggest an overall grain imbrication with a gentle easterly dip of  $7^\circ$ , or at direction opposite to that indicated by

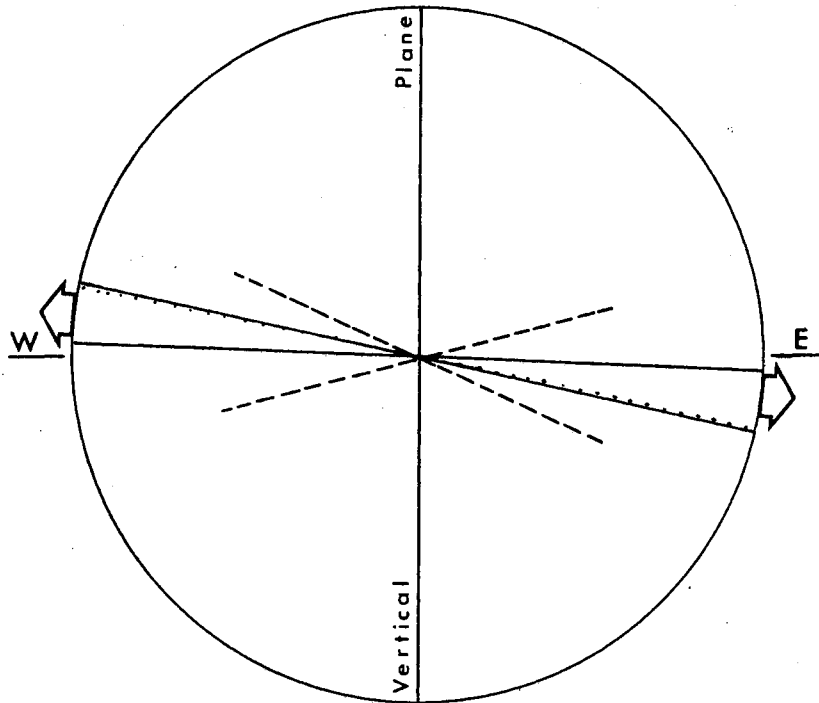


Figure 6. Diagram showing imbrication in the lowermost unit of the Eagle Sandstone. Dashed lines are results from thin sections; solid line is COBRA measurement; and dotted line is DA measurement. Overall weighted average shows an imbrication of  $7^\circ$  to the east. Length of the line corresponds to quality of results.

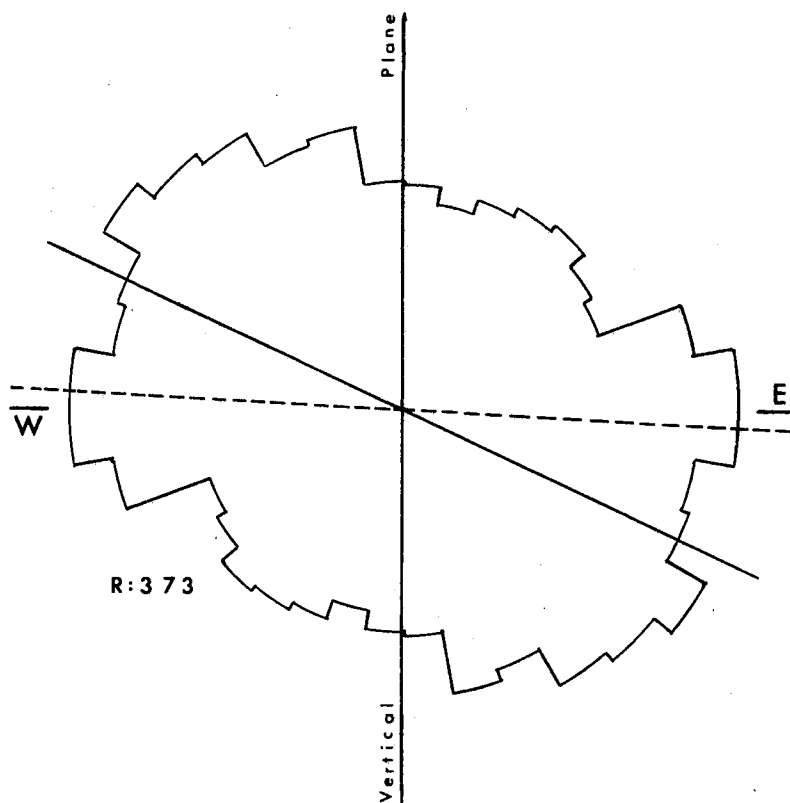


Figure 7. Grain imbrication in Eagle Sandstone (sample 106).  $R$  = total number of grains measured. A  $30^\circ$ -sliding average was used in preparation of diagram. Solid line dipping  $25^\circ$  eastward is calculated preferred direction, using Chayes' minimum variance fabric mean. Dashed line is COBRA measurement.

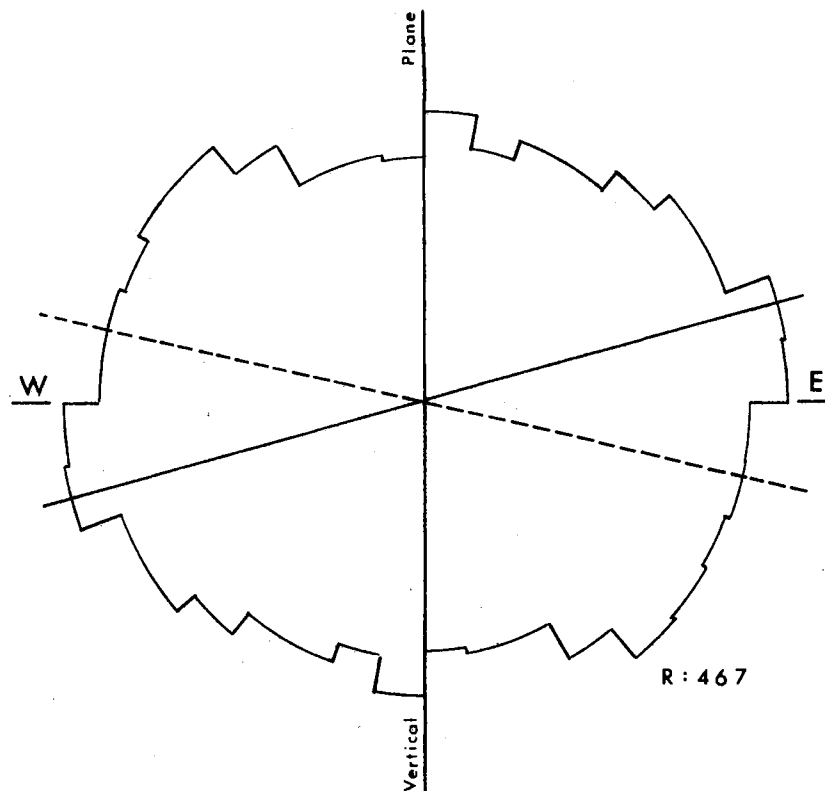


Figure 8. Grain imbrication in Eagle Sandstone (sample 97). R = total number of grains measured. A 30°-sliding average was used in preparation of diagram. Solid line dipping 15° westward is calculated preferred direction, using Chayes' minimum variance fabric mean. Dashed line is DA measurement.

TABLE II

## Grain Imbrication in Lowermost Unit Eagle Sandstone

Sample No.	No. Plugs	No. Grains	Range In Measurements	Results	Quality <sup>1</sup>
106-I	4	--	13°	3°E	E
106-TS <sup>2</sup>	-	373	--	25°E	F
97-TS <sup>2</sup>	-	467	--	15°W	F
97-DA <sup>3</sup>	5	--	10°	13°E	E

<sup>1</sup>See Appendix E for ratings of quality of results. E = Excellent, G = Good, F = Fair.

<sup>2</sup>TS - Thin Section Measurement

<sup>3</sup>DA - Dielectric Anisotropy Measurement

Shelton and Mack (1970). The gentle dip measured by the COBRA instrument and the wide range in the orientation of individual grains observed in thin section suggest that both backwash and wash were operative during deposition but that the backwash was somewhat more dominant. Another possible source for the variation in measurements is undetected bioturbation in the massively bedded samples. Galveston Island, to which the lowermost Eagle unit has been compared (Shelton, 1965), also shows imbrication opposite to the direction of accretion. A more extensive study is required for a greater degree of certainty concerning Eagle grain imbrication, and radiographs are needed to determine those samples which are not bioturbated and therefore best suited for analysis.

## CHAPTER IV

### GRAIN ORIENTATION IN SHALLOW MARINE- SHOREFACE DEPOSITS

The Ordovician Harding Sandstone in Colorado, the Ordovician Burgen Sandstone in Oklahoma, and the Cretaceous Trinidad Sandstone in Colorado are horizontally bedded, and all three are considered to represent shallow marine to shoreface environments. In the study of each sandstone, three-dimensional grain orientation, including imbrication, was used to determine the predominant depositing current.

#### Harding Sandstone

##### Stratigraphic Framework

The Ordovician Harding Sandstone crops out in the area of central Colorado around Canon City. It overlies the Manitou Formation disconformably and is overlain unconformably by the Fremont Formation, except where the Fremont has been removed by post-Ordovician erosion.

The Harding Sandstone ranges in thickness from 0 to 186 ft.; most of the variation is thought to reflect post-depositional erosion. The Harding is characterized by bioturbation and horizontal beds. It contains numerous ostracoderm plates. Except for a thin basal unit, which is coarse-grained, the Harding is generally a very-fine to fine-grained and well- to very-well sorted sandstone with varying

amounts of interbedded shale. In the northwest, the Harding is greater than 80 percent sand, whereas in the southeast, sand composes only 20 to 40 percent of the formation (Figure 9).

The underlying Manitou Formation ranges in thickness from 0 to 50 ft. in this area. It consists of thin-bedded, red to pink, dolomitic limestone and chert.

The Fremont Formation ranges up to 300 ft. thick, with post-depositional erosion being responsible for most of the variation in thickness. It is a pink to light buff, coarse-grained, massive dolomite and limestone, which contain little silt and clay.

#### Depositional Environment and Trend

The abundant ostracoderm remains, bioturbation, horizontal bedding, uniform grain size, good sorting, and regional lithofacies suggest that the Harding was deposited in a shallow marine environment on a stable shelf. Although the trend, inferred from an isopach map of the Harding Sandstone prepared by Sweet (1954), is  $N60^{\circ}E$ , it is thought that the present thicknesses reflect only the erosional remnants of the Harding. Therefore, the trend of  $N20^{\circ}E$ , derived from a study of lithofacies by Foster (1972), is thought to be representative of depositional conditions. The direction of decreasing sand is regarded as portraying the direction of increasing distance from shoreline.

#### Grain Orientation

Four samples were collected in the vicinity of Canon City, Colorado, and from them 18 plugs were drilled. Good results were obtained in one sample, fair results in another, and unacceptable



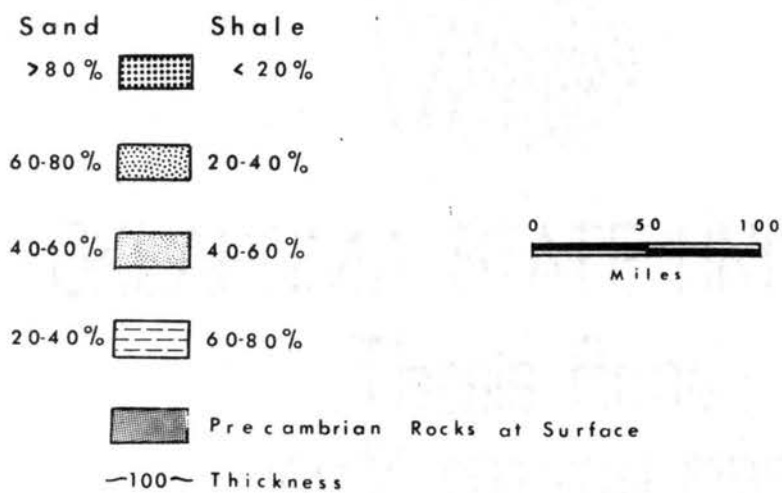
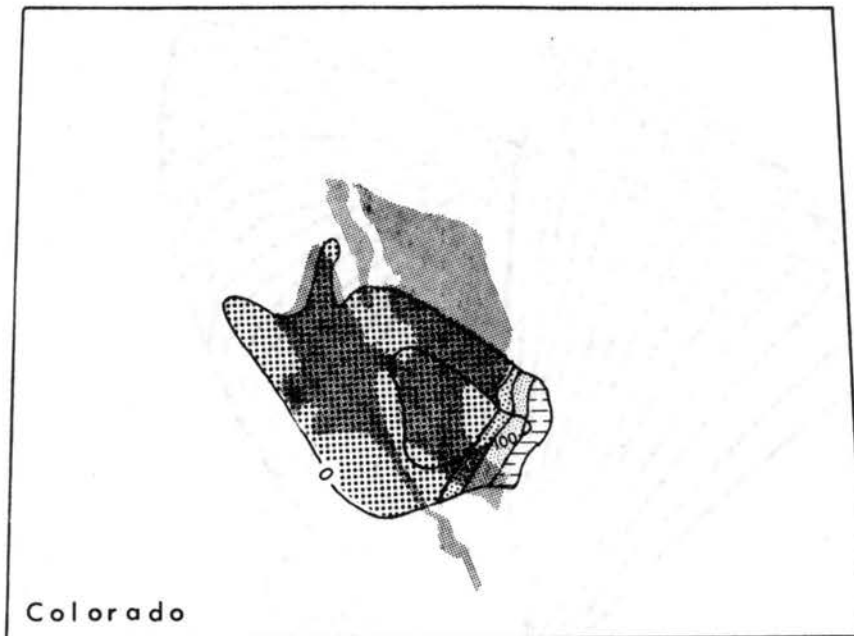


Figure 9. Lithofacies and reconstructed isopach map of the Harding Sandstone in Colorado. A trend of  $N20^{\circ}E$  is suggested from the lithofacies map. (From Foster, 1972).

results were obtained in the others. Bioturbation in the 2 unacceptable samples is thought to be largely responsible for the spurious measurements. Also included in the study are 4 samples, (H-5 through H-8), which were previously analyzed in the sedimentology laboratory at Oklahoma State University. The average grain orientation, for all of the samples with usable results, is N65°W, or 83° from the lithofacies trend (Table III; Figure 10).

TABLE III  
Grain Orientation in Harding Sandstone

Sample No.	No. Plugs	Range In Measurements	Results	Quality <sup>1</sup>
H-1	4	44°	N73°W	G
H-2	5	75°	N71°E	F
H-3	4	100°	--	NG
H-4	5	104°	--	NG
H-5	2	10°	N13°E	G
H-6	2	10°	N55°W	G
H-7	2	10°	N55°W	G
H-8	3	40°	N85°W	G

<sup>1</sup>See Appendix E for rating of quality of results.  
G = Good, F = Fair, NG = No Good.

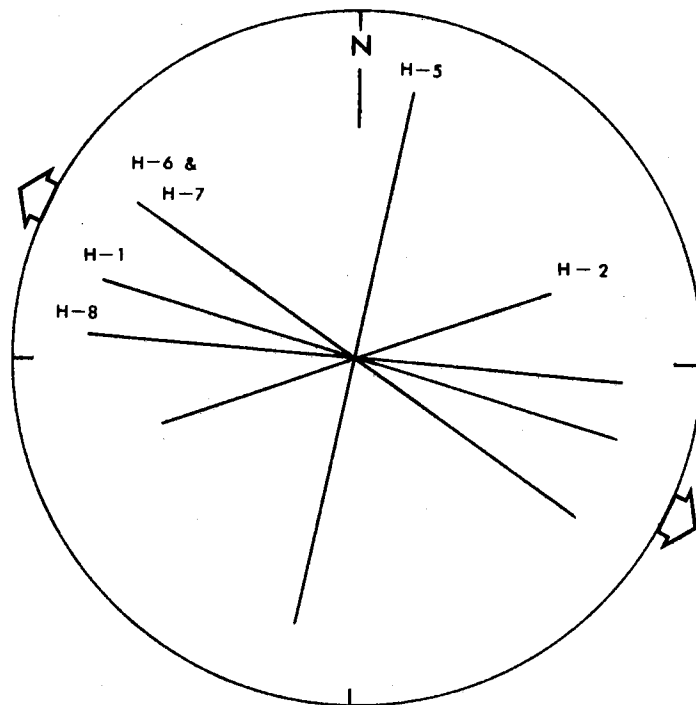


Figure 10. Grain orientation in Harding Sandstone, showing an average direction of  $N65^{\circ}W$ . Results for H-5 are not included in calculation of average direction. Length of line corresponds to quality of results.

From analysis of 5 plugs of sample H-1, the grains show imbrication toward the east-southeast at an average angle of  $8^{\circ}$  (Figure 11). The quality of the data is excellent; the range is only  $6^{\circ}$  in the 5 plugs.

Grain orientation is approximately perpendicular to the trend of the overall sand body, and the east-southeast imbrication suggests that the wave-related currents moving shoreward were the dominant depositional process in the Harding Sandstone. One sample, H-5, shows grain orientation almost parallel with the lithofacies trend of Foster (1972). This phenomenon is thought to be the result of longshore currents. A more extensive study of grain orientation is recommended for a better delineation of Harding paleocurrents and depositional trends.

### Burgen Sandstone

#### Stratigraphic Framework

The Burgen Sandstone crops out in northeastern Oklahoma on the southwestern flank of the Ozark uplift. It unconformably overlies the Cotter Dolomite and is overlain conformably by the Tyner Formation. The Burgen locally fills sinks and caverns, formed by post-Cotter solution, with massively bedded sandstone (Gore, 1952). The three formations, all of which are Ordovician in age, thin rapidly northward by truncation (Huffman, et al., 1966).

The Burgen Sandstone ranges in thickness from 0 to 100 ft. Exposed thickness is 43 ft. at the Tahlequah location and 23 ft. at the Locust Grove location. Generally, it is a massively or

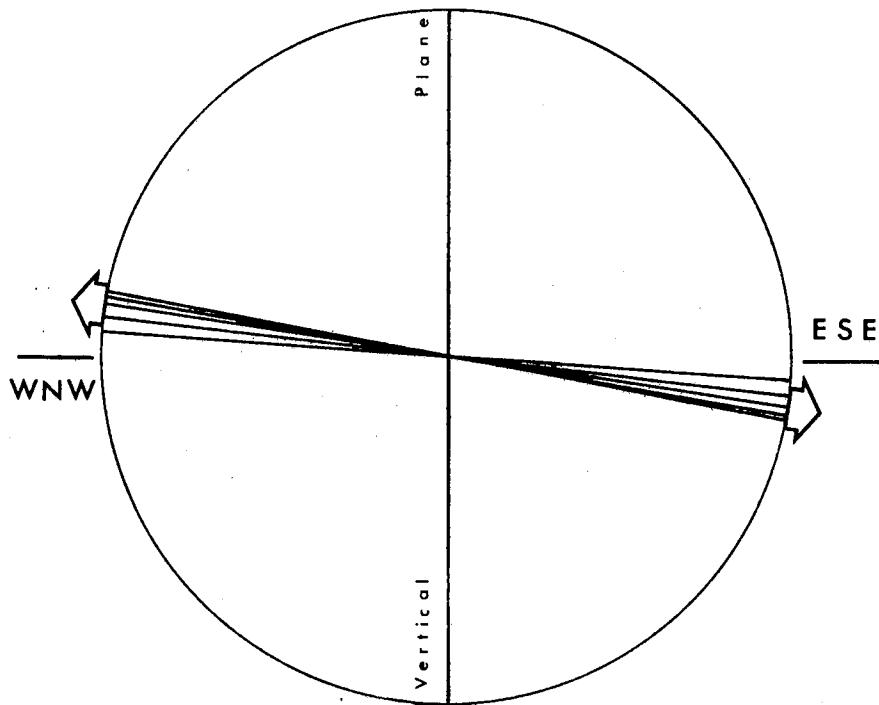


Figure 11. Grain imbrication in Harding Sandstone (sample H-1) is at an angle of  $8^\circ$  to the east-southeast. Each line represents a measurement in one plug.

horizontally bedded sandstone which alternates with thin beds of shale, limestone, and dolomitic limestone. The grains range from fine to medium and are angular to well-rounded, commonly showing secondary enlargement, pitting, etching, and frosting (Huffman, 1966). The cement is calcareous in the lower units and siliceous in the upper beds, with iron-oxide stain characterizing the whole sandstone body.

The underlying Cotter Dolomite ranges in thickness from 0 to 270 ft. and consists of thick-bedded, finely crystalline dolomite. Occasional thin beds of sandstone, shale, chert, and intraformational conglomerates are also present (Huffman, 1958).

The Tyner Formation varies in thickness from 0 to 100 ft. (Stark, 1961) and consists of a lower sandy dolomite and green, waxy shale, a middle bright green shale, and an upper cherty, very finely crystalline, dolomitic limestone (Cram, 1932).

#### Depositional Environment and Trend

The Burgen Sandstone probably formed as a nearshore shallow marine to strandline, or barrier-bar, deposit near the edge of the Ozark uplift which existed during Ordovician time (Figure 12). Submergence of the Ozark uplift resulted in the deposition of Tyner shales and limestones conformably on the Burgen Sandstone. Subsequent uplift and erosion do not permit determination of the original extent of the Burgen.

#### Grain Orientation

Twenty-four plugs were drilled from 5 samples, 2 collected near Locust Grove and 3 collected near Tahlequah (Figure 12). Good results were obtained in 2 samples, fair results in 1, and poor

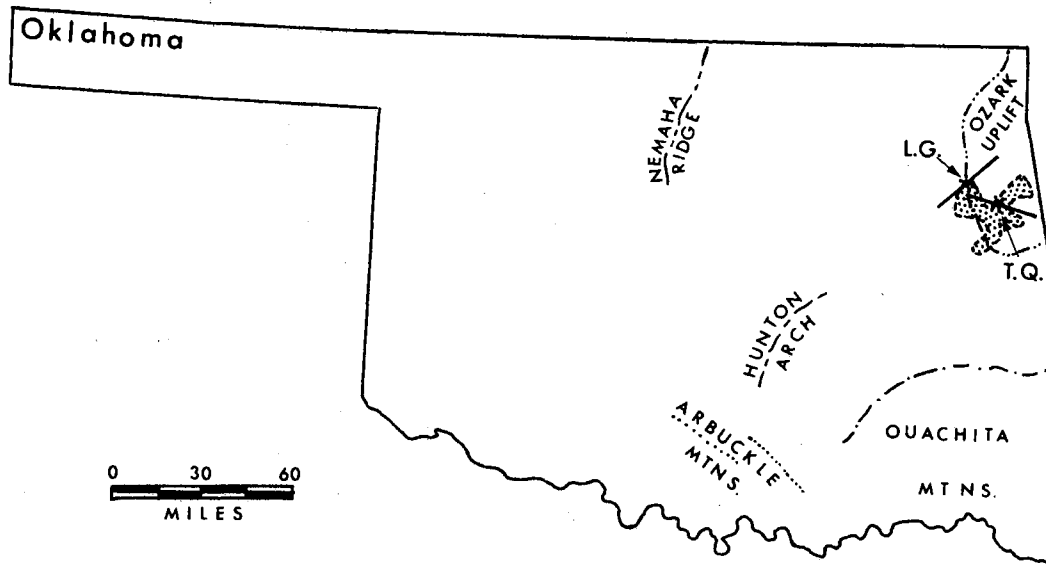


Figure 12. Location map showing area of outcrop of Burgen Sandstone and sample localities. TQ = Tahlequah location; LG = Locust Grove location. Average grain orientation forms a high angle to the southwest flank of the Ozark uplift.

results in the remaining 2. The average grain orientation for the Locust Grove area is  $N44^{\circ}E-S44^{\circ}W$  and  $N73^{\circ}W-S73^{\circ}E$  for the Tahlequah area. The overall average is  $N82^{\circ}E-S82^{\circ}W$  (Table IV, Figure 13).

TABLE IV  
Grain Orientation in Burgen Sandstone

Sample No.	No. Plugs	Range In Measurements	Results	Quality <sup>1</sup>
TQ-1	5	$83^{\circ}$	$N62^{\circ}W-S62^{\circ}E$	P
TQ-2	5	$59^{\circ}$	$N87^{\circ}E-S87^{\circ}W$	G
TQ-3	5	$62^{\circ}$	$N63^{\circ}W-S63^{\circ}E$	F
LG-1	5	$53^{\circ}$	$N53^{\circ}E-S53^{\circ}W$	G
LG-2	4	$78^{\circ}$	$N35^{\circ}E-S35^{\circ}W$	P

<sup>1</sup>See Appendix E for rating of quality of results. G = Good, F = Fair, P = Poor.

The range in average grain orientation per sample is  $31^{\circ}$  for the Tahlequah samples, whereas the range is  $18^{\circ}$  for the Locust Grove samples. Grains in sample TQ-2 are imbricated toward the east at an average angle of  $18^{\circ}$  (Figure 14). The quality of the data is excellent with a range of  $36^{\circ}$  in the 5 plugs, which were drilled perpendicular to grain orientation.

Because grain orientation lies at a high angle to the sandstone trend on the west flank of the Ozark uplift and low-angle initial dip



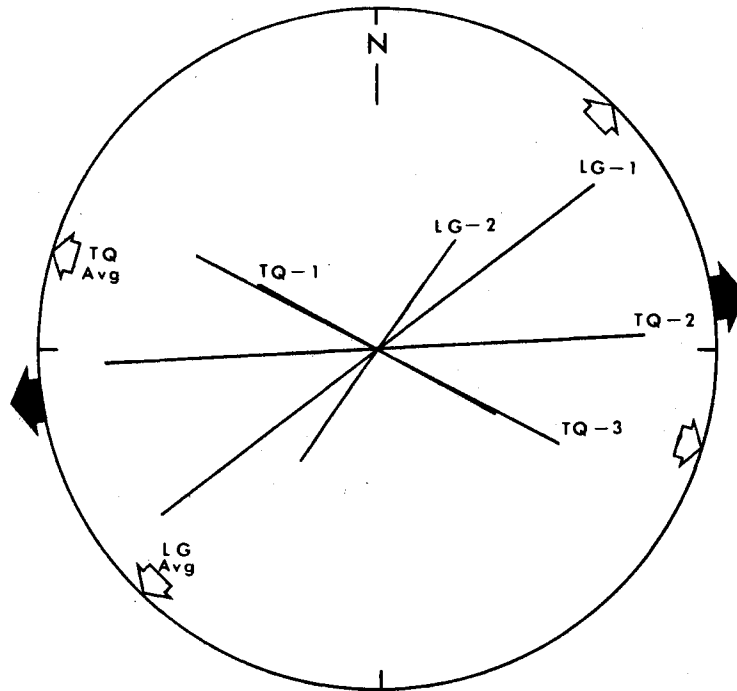


Figure 13. Grain orientation in Burgen Sandstone. Average orientation for Tahlequah samples is  $N73^{\circ}W-S73^{\circ}E$ ; average for Locust Grove is  $N44^{\circ}E-S44^{\circ}W$ ; and overall average is  $N82^{\circ}E-S82^{\circ}W$ . Symbols and numbers refer to samples. TQ = Tahlequah location and LG = Locust Grove location. Length of line corresponds to quality of results.

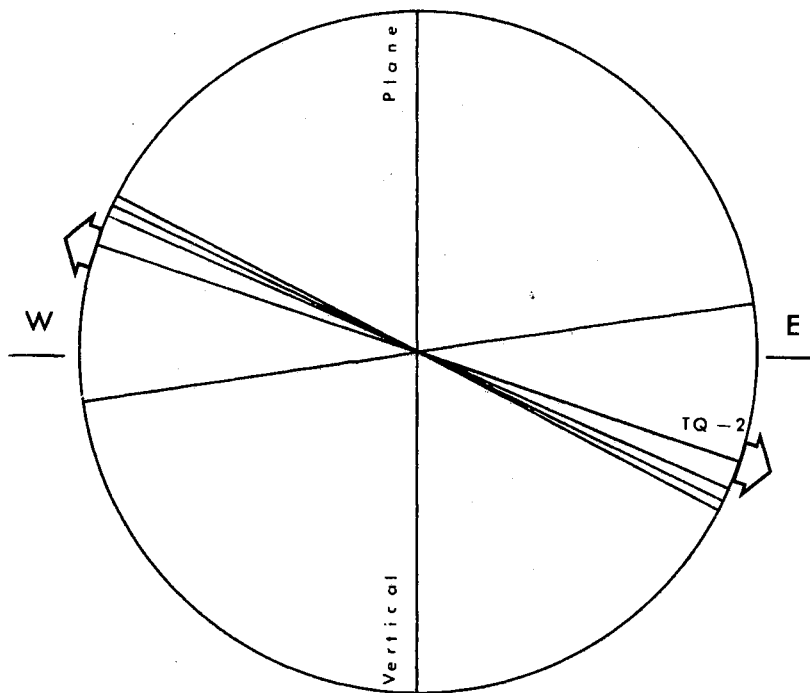


Figure 14. Grains in Burgen Sandstone are imbricated  $18^\circ$  to the east. Each line represents a measurement in 1 plug.

at the Tahlequah location is in a S70°W direction, it is thought that wave-related currents were the dominant depositing agent. Grain imbrication to the east, or shoreward, suggests they were deposited by backwash.

### Trinidad Sandstone

#### Stratigraphic Framework

The Upper Cretaceous Trinidad Sandstone occurs in a linear band trending northwest-southeast across southeastern Colorado and northeastern New Mexico, principally in the Canon City embayment and the Raton basin (Figure 15). The Trinidad Sandstone overlies the Pierre Shale and underlies the Vermejo Formation. It varies in thickness from 76 to 300 ft. in the Raton basin (Matuszczak, 1969; Johnson and Wood, 1956) and from 100 to 200 ft. in the Canon City area and is composed of buff to gray sandstone with thin interbeds of light tan to gray silty shale. The unit generally contains horizontal bedding but small-scale cross-bedding, medium-scale cross-bedding, parting lamination, and burrowing are also present (Matuszczak, 1969). The average grain size is predominantly fine-grained with a range from very fine- to medium-grained.

The Pierre Shale ranges in thickness from about 3500 ft. in the Canon City area (DeFord, 1929) to about 2300 ft. in the Raton basin (Johnson and Wood, 1956). The lower part is chiefly a dark gray to nearly black, noncalcareous shale, whereas the upper zone consists of buff to gray, thin-bedded, fine-grained sandstone interbedded with thin beds of gray to dark gray, silty and sandy shale (Johnson and Wood,

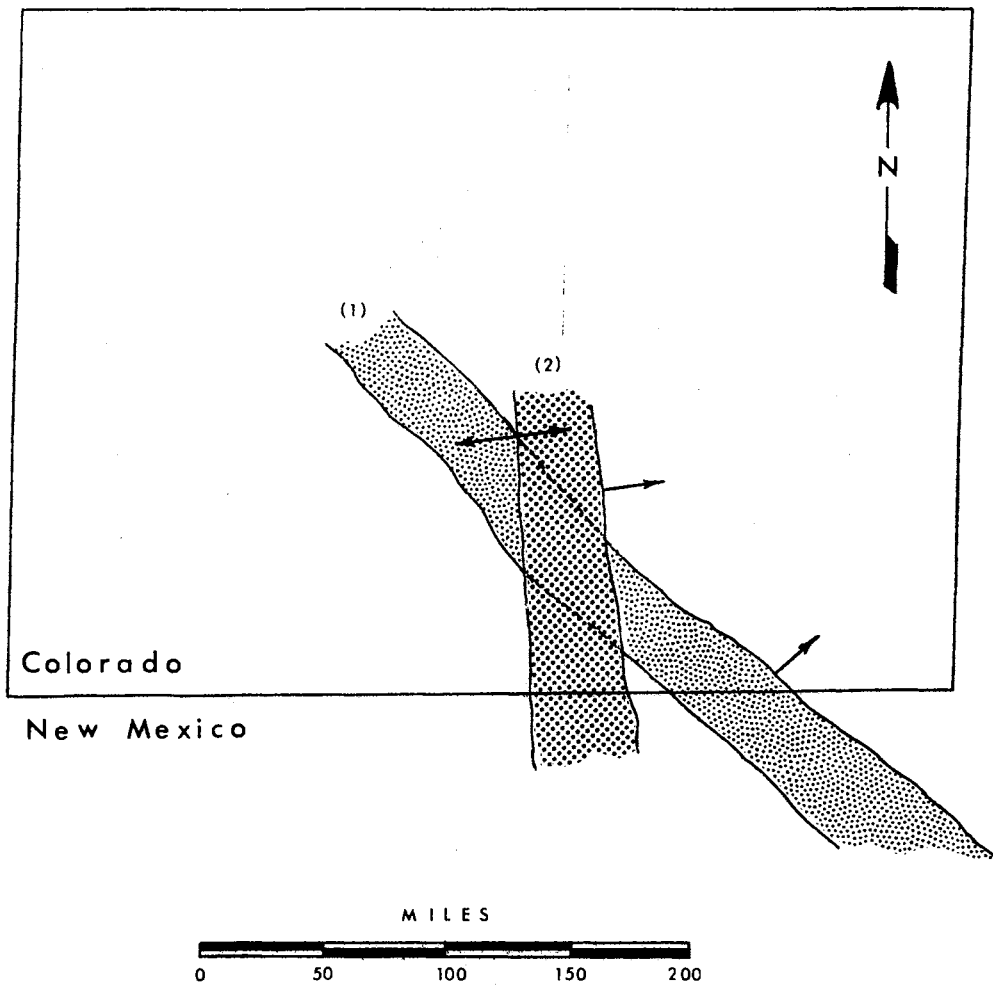


Figure 15. Regional trend of Trinidad Sandstone. Trend (1), of  $N50^{\circ}W$ , is from McGookey (1972) and trend (2), of  $N10^{\circ}W$ , is from Johnson and Wood (1956). Grain orientation is  $N77^{\circ}E$ , a direction which is perpendicular to trend (2) but  $60^{\circ}$  from trend (1). Single arrows indicate postulated regression directions.

1956). These upper beds tend to intertongue with the lower beds of the Trinidad. This transition zone is commonly 40 to 80 ft. thick (Matuszczak, 1969).

The Vermejo of the Raton basin includes 550 ft. of buff to grayish-green, slightly arkosic sandstone, buff to dark gray siltstone, carbonaceous, coaly and silty shale, and many coal lenses (Johnson and Wood, 1956). The Vermejo, in the Canon City area, is similar in lithology and increases in thickness to approximately 1000 ft. (DeFord, 1929).

#### Depositional Environment and Trend Indicators

The Pierre Shale represents regressive marine deposition, with a progressive shallowing of water depths upward. The formation was probably deposited almost entirely in shallow marine waters. However, the lower part of the Pierre Shale may have been deposited in relatively deep water if depositional conditions were similar to those for certain Upper Cretaceous shales of Wyoming (Asquith, 1970). Progressive shallowing continued during deposition of the Trinidad. It was deposited as shallow marine-shoreface sand, or even barrier-bar sand at or near the shoreline (Weimer, 1960). Marsh and swamp conditions were prominent during deposition of the Vermejo, as regressive conditions resulted in final withdrawal of marine waters during the Cretaceous (Johnson and Wood, 1956).

Several workers have estimated shoreline trends and regression directions for the Upper Cretaceous, and for the Trinidad in particular. Johnson and Wood (1956) show a shoreline trend of N10°W, from which a regression direction is inferred to be N80°E (Figure 15). From

ripple marks, heavy mineral lenses, thick coal lenses, and supplementary thickness data, Matuszczak (1969) estimated the shoreline trend to be approximately N75°W and the regression direction as north-northeast. The N50°W direction determined by McGookey (1972) was made from analysis of the work by Gill and Cobban (1969) (Figure 15). Several paleocurrent indicators measured on outcrop in the Canon City area as a part of this study show an average direction of N80°-90°E.

#### Grain Orientation

Four samples were obtained from an outcrop section east of Canon City, and measurements were made of directional conductivity in 19 plugs. Results are excellent in 3 samples and good in the other. The average paleocurrent direction is N77°E, with a range in measurements of 96° from N33°E to S51°E (Table V; Figure 16).

TABLE V

#### Grain Orientation in Trinidad Sandstone

Sample No.	No. Plugs	Range In Measurements	Results	Quality <sup>1</sup>
T-1	5	57°	N33°E	G
T-2	5	29°	N60°E	E
T-3	5	22°	S51°E	E
T-5	4	10°	S88°E	E

<sup>1</sup>See Appendix E for rating of quality of results.  
E = Excellent, G = Good, F = Fair.

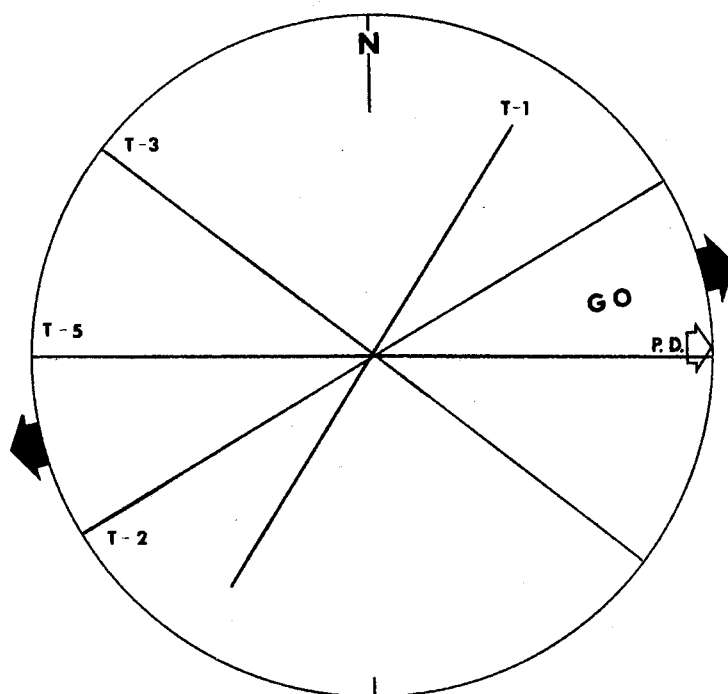


Figure 16. Grain orientation in Trinidad Sandstone, showing an average direction of  $N77^{\circ}E$ . Length of line corresponds to quality of results.

Plugs from samples T-2 and T-5 were drilled perpendicular to the geographic direction of grain orientation for determination of grain imbrication. Both samples, with excellent results, show an imbrication direction to the west-southwest (Table VI; Figure 17).

TABLE VI

## Grain Imbrication in the Trinidad Sandstone

Sample No.	No. Plugs	Range In Measurements	Results	Quality <sup>1</sup>
T-2	4	15°	10°WSW	E
T-5	5	10°	11°WSW	E

<sup>1</sup>See Appendix E for rating of quality of results.  
E = Excellent, G = Good, F = Fair.

The preferred grain orientation in the Trinidad Sandstone is approximately perpendicular to the sand-body trend postulated by Johnson and Wood, but 60° to the trend of McGookey. The high angle between grain orientation and the sand trend suggests deposition by waves rather than longshore currents. Imbrication to the west-southwest suggest that backwash, rather than wash from the waves breaking westward against the shoreface, was dominant during deposition. A similar relationship is thought to exist at Galveston Island and in the lowermost unit of the Eagle Sandstone.



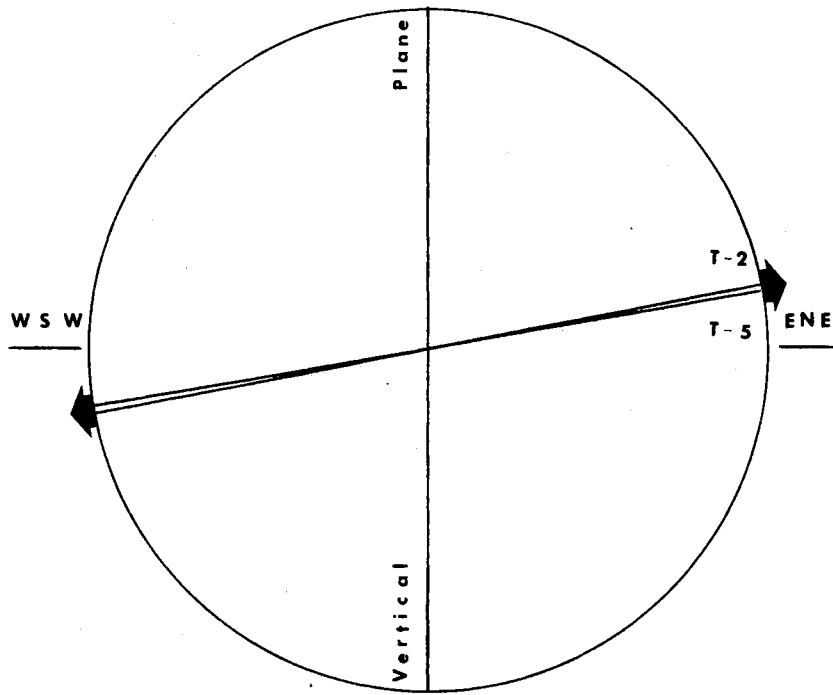


Figure 17. Grains in Trinidad Sandstone are imbricated  $10^{\circ}$  west-southwest. Each line represents the average for each sample.

## CHAPTER V

### GRAIN ORIENTATION IN DELTAIC DEPOSITS:

#### VAMOOSA FORMATION

One diagnostic feature of deltaic deposits is the wide range in paleocurrent indicators because of variation in depositional processes and their orientation. Grain orientation is compared to other paleocurrent indicators in one subdivision of the Vamoosa Formation, and changes in grain orientation are related to changes in possible source areas with time.

#### Stratigraphic Framework

The Vamoosa Formation, Upper Pennsylvanian in age, is present in Oklahoma north of the Arbuckle and Wichita uplifts and extends into southern Kansas (Figure 18). It crops out along the eastern margin in a north-northeasterly trending band, from Pontotoc County in the south to Osage County in the north. It consists of a sequence of sandstone and shale, with conglomerate best developed at the base (Oakes, 1959).

Sedimentary structures in the sandstone bodies include massive bedding, small- and medium-scale cross-bedding, initial dip, and horizontal bedding. Grain size most commonly ranges from fine- to medium-grained. Colors are red, brown, reddish-brown, buff, and white. Sandstones range in composition from subarkoses to quartzarenites, but

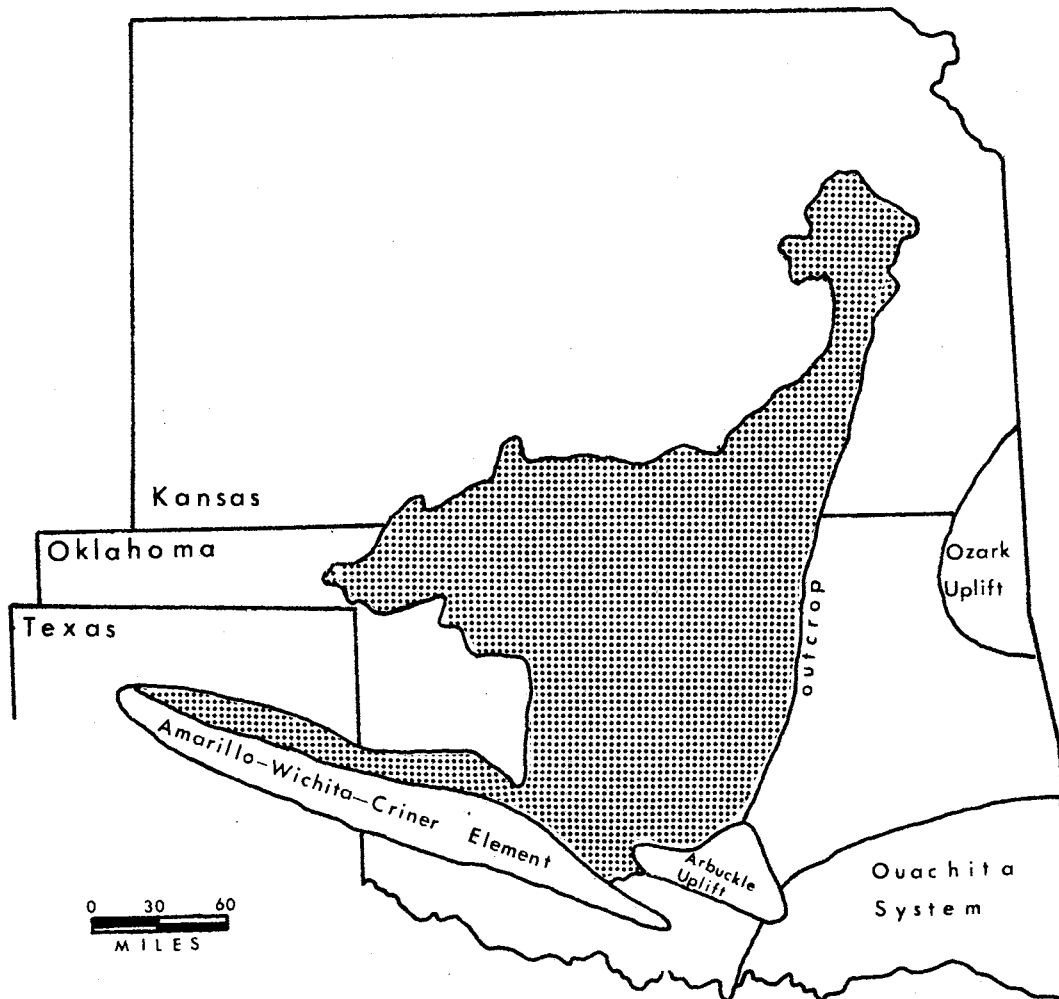


Figure 18. Sand distribution map of Vamoosa Formation (stippled) in Oklahoma, Kansas, and Texas, showing depositional extent and possible source areas, during maximum regression.

are predominantly sublitharenites (Terrell, 1972). Silica cement is prominent, but some calcite is also present (Oakes, 1959).

The following are formational characteristics of the Vamoosa on outcrop:

1. Thinning of 10 ft. per mi. occurs away from Okfuskee County, where it reaches a maximum thickness of approximately 700 ft. (Ries, 1954). The Vamoosa also shows a westward thickening of about 12 ft. per mi. (Tanner, 1956).

2. Shale, which is varied in color, becomes more abundant in a northward direction.

3. Pebbles in the conglomeratic section are coarsest in Seminole and Okfuskee County (Levorsen, 1930). The basal conglomerate is not present north of central Creek County (Greig, 1959). Sandstone members are characterized by rapid lateral variation (Levorsen, 1930 and Greig, 1959).

4. Average particle size decreases to the north (Tanner, 1956).

Vamoosa sandstones have been studied in some detail in Creek, Pawnee, and Osage Counties, where the formation has been divided into 4 unnamed units. In this thesis they are referred to as the lower, lower middle, upper middle (Elgin), and upper units.

The Lecompton Limestone member of the Pawhuska Formation overlies the Vamoosa Formation conformably whereas the Tallant Formation underlies the Vamoosa unconformably. In the southern part of its area of development, the Vamoosa is overlain unconformably by the Ada Formation, which truncates the Lecompton Limestone (Oakes, 1959).

### Depositional Environment and Trend

Due to the formational characteristics of the Vamoosa Formation, numerous authors have postulated that it was deposited in a north-retreating sea. The Arbuckle and Ouachita uplifts, to the south and southeast, respectively, have been considered as major source areas. According to Terrell (1972), the Ozark uplift to the east may have supplied a minor amount of sediments. Tanner (1956) suggests that the source area is to the south but not to the southeast.

Ries (1954) is of the opinion that the sandstone lenses, with irregular distribution and thickness, represent a sequence of deltaic facies. Tanner (1956), on the other hand, believes the Vamoosa to be the product of a beach or offshore bar. Terrell (1972) concludes that the Elgin Sandstone Member of the Vamoosa Formation was deposited primarily as distributary and alluvial bodies, with minor development of delta-fringe and shallow marine units.

### Grain Orientation

A total of 88 measurements have been made of grain orientation in Vamoosa sandstones, representing all 4 subdivisions. Some of these measurements were made by Terrell (1972) and D. E. Mack. The DA instrument was used by Mack; the COBRA was used by Terrell and in this study. The lower unit shows a primary trend of  $N15^{\circ}W-S15^{\circ}E$  and a secondary trend of  $N75^{\circ}W-S75^{\circ}E$  (Figure 19), whereas the lower middle unit shows a primary trend of  $N25^{\circ}E-S25^{\circ}W$  and a secondary trend of  $N75^{\circ}W-S75^{\circ}E$  (Figure 20). The upper middle unit and the upper units

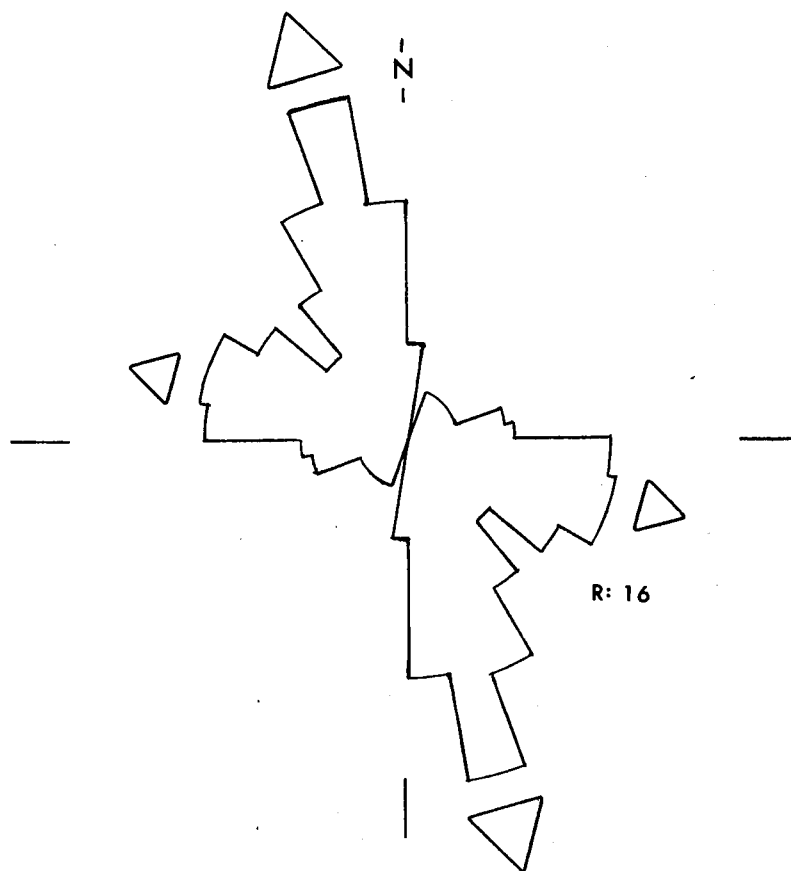


Figure 19. Weighted average grain orientation in the lower unit of the Vamoosa Formation, indicating a primary trend of  $N15^{\circ}W-S15^{\circ}E$  and a secondary trend of  $N75^{\circ}W-S75^{\circ}E$ . A  $30^{\circ}$ -sliding average and the quality of measurements were used in preparation of the diagram.

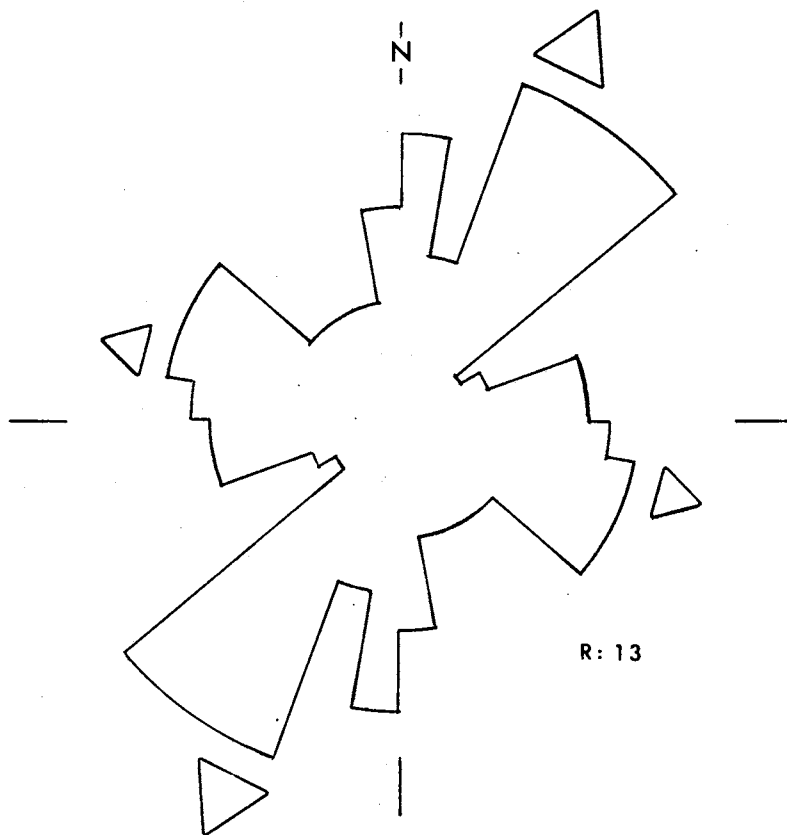


Figure 20. Weighted average grain orientation in the lower middle unit of the Vamoosa Formation, indicating a primary direction of  $N25^{\circ}E-S25^{\circ}W$  and a secondary direction of  $N75^{\circ}W-S75^{\circ}E$ . Method of preparation is given with Figure 19.

have preferred orientations of  $N70^{\circ}W-S70^{\circ}E$  and  $N80^{\circ}W-S80^{\circ}E$ , respectively (Figures 21 and 22). The overall average grain orientation for Vamoosa sandstones is  $N70^{\circ}W-S70^{\circ}E$  (Figure 23). The data are tabulated in Table VII.

TABLE VII

## Grain Orientation in the Vamoosa Formation

Subdivision	Number of Measurements	Quality <sup>1</sup> of Results					Primary Trend	Secondary Trend
		E	G	F	P	NG		
Upper	37	18	9	5	4	1	$N80^{\circ}W-S80^{\circ}E$	
Upper Middle (Elgin)	19	14	3	2	0	0	$N70^{\circ}W-S70^{\circ}E$	
Lower Middle	16	5	3	3	2	3	$N25^{\circ}E-S25^{\circ}W$	$N75^{\circ}W-S75^{\circ}E$
Lower	16	7	6	3	0	0	$N15^{\circ}W-S15^{\circ}E$	$N75^{\circ}W-S75^{\circ}E$
Total	88	44	21	13	6	4	$N70^{\circ}W-S70^{\circ}E$	

<sup>1</sup>See Appendix E for quality of results per sample. E = Excellent, G = Good, F = Fair, P = Poor, and NG = No Good.

The secondary trends and the rather wide range in measurements suggest sandstones representing several subenvironments of the deltaic complex were analyzed. Diversity in measurements is believed to be the result of changing paleoslope and deposition paralleling paleoslope by longshore currents.



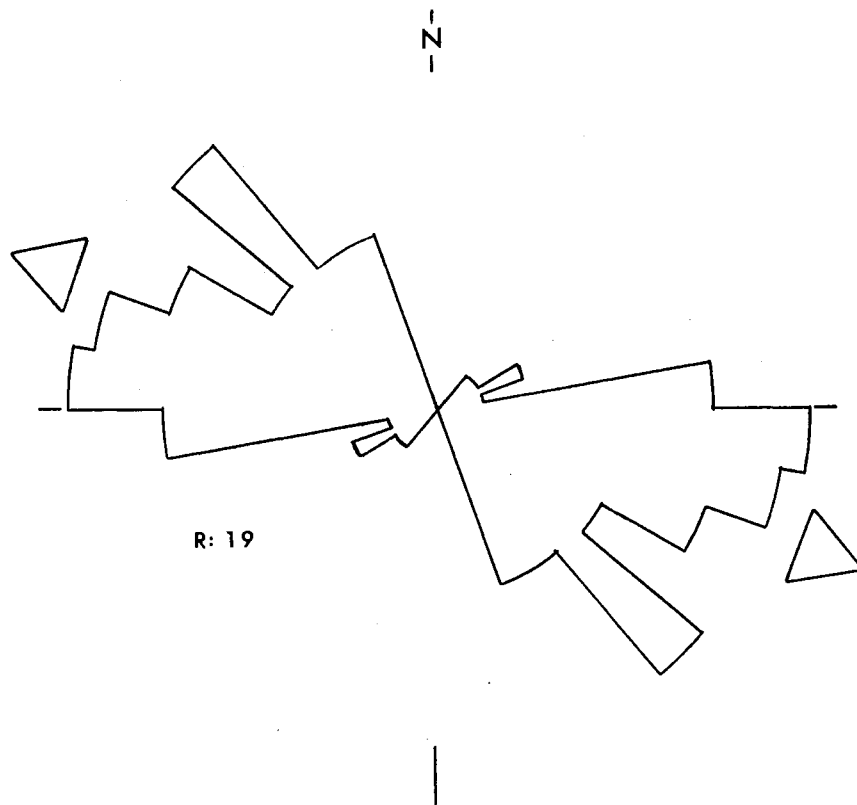


Figure 21. Weighted average grain orientation in the upper middle unit (Elgin Sandstone Member) of the Vamoosa Formation shows a primary direction of  $N70^{\circ}W-S70^{\circ}E$ . Method of preparation is given with Figure 19.

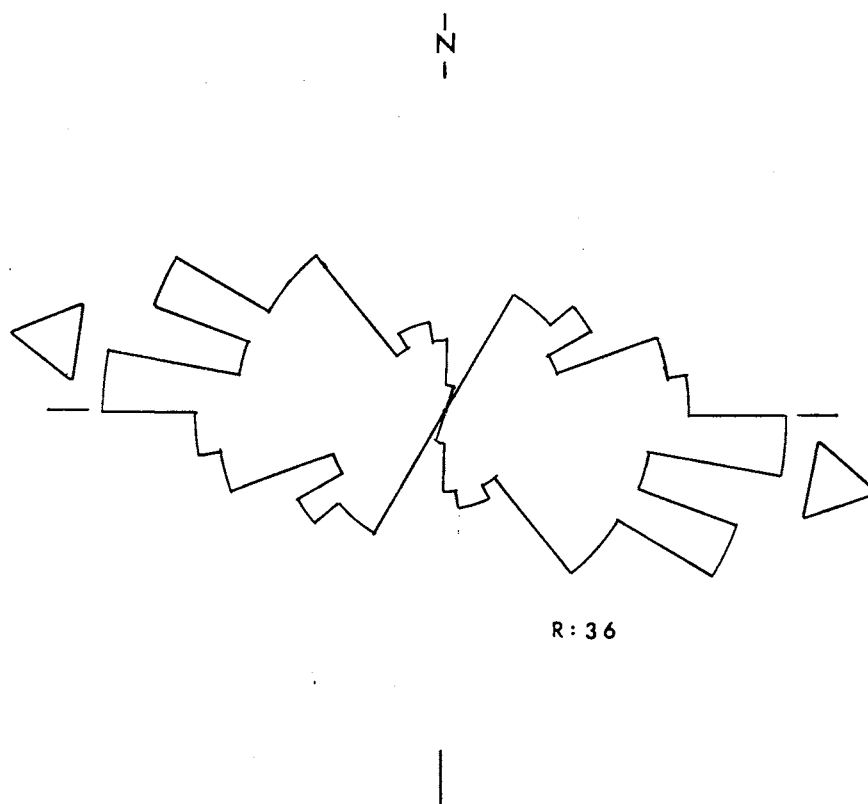


Figure 22. Weighted average grain orientation in the upper unit of the Vamoosa Formation, with a trend of  $N80^{\circ}W-S80^{\circ}E$ . Method of preparation is given with Figure 19.

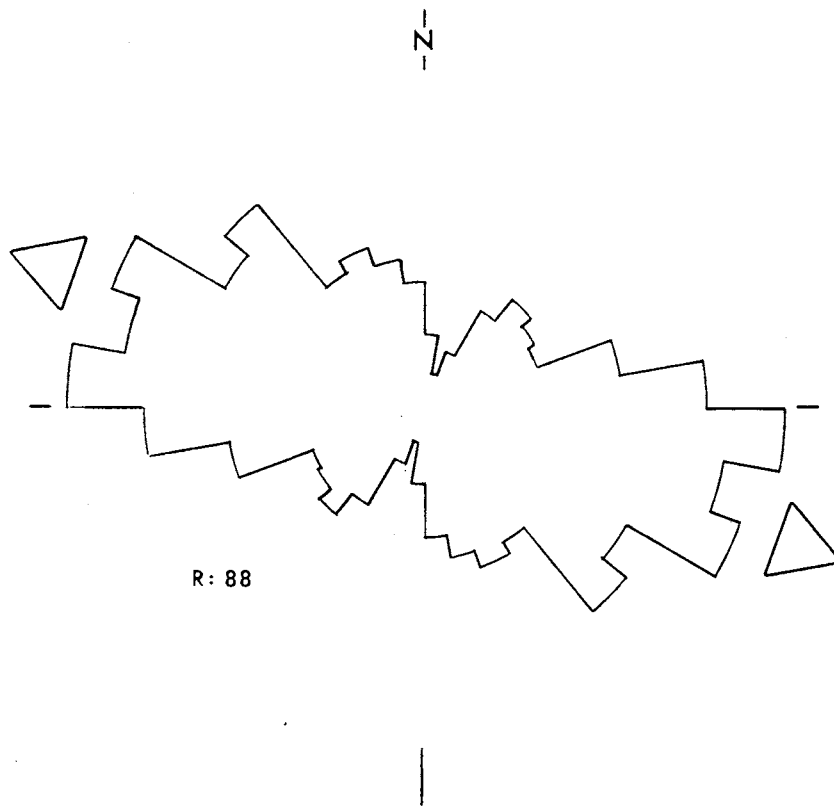


Figure 23. Composite weighted average grain orientation in Vamoosa Sandstones indicates a preferred direction of  $N70^{\circ}W-S70^{\circ}E$ . Method of preparation is given with Figure 19.

### Correlation of Grain Orientation and Paleocurrents

Various paleocurrent indicators have been measured in the Elgin Member of the Vamoosa Formation (Terrell, 1972). They include medium-scale cross-bedding, initial dip, parting lineation, small-scale cross-bedding, ripple marks, and cut-outs; a total of 281 measurements were made. These paleocurrent indicators show a preferred trend of N40°W-S40°E, compared to a trend of N70°W-S70°E for grain orientation in 19 samples (Figure 24). Channel or distributary sandstones in the Elgin show a current direction of N35°W, whereas delta-fringe sandstones show a primary direction of N50°W and a secondary trend of N40°E-S40°W (Terrell, 1972).

### Change in Grain Orientation With Time

An overall westerly change in grain orientation in younger sandstones (Figure 25) suggests a possible change in dominant source areas, which are as follows:

1. Arbuckle and Ouachita uplifts for the lower unit.
2. Arbuckle uplift as source for lower middle unit.
3. Ouachita uplift, with some possible influence from the Ozark uplift or Appalachian system for the upper middle unit (Elgin Sandstone).
4. Ozark uplift or Appalachian system for upper unit.

For a more sophisticated interpretation of Vamoosa grain orientation, it is suggested that additional subdivisions be made according to depositional environment.

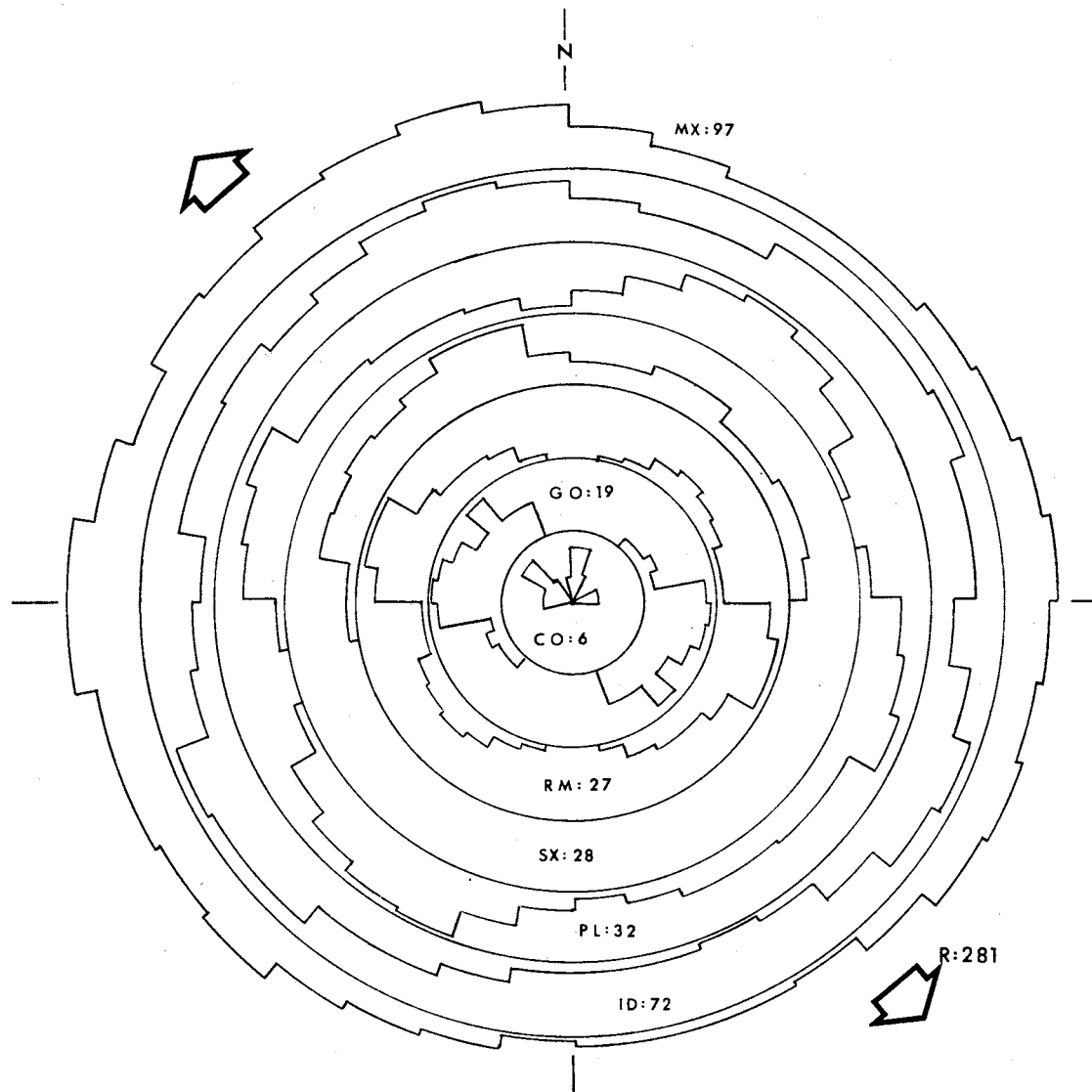


Figure 24. Rose diagram for paleocurrent indicators with overall trend of  $N40^{\circ}W-S40^{\circ}E$  and grain orientation with trend of  $N70^{\circ}W-S70^{\circ}E$  in the Elgin Sandstone (Upper Middle Unit). CO = cut-out, GO = grain orientation, RM = ripple marks, SX = small-scale cross-bedding, PL = parting lineation, ID = initial dip, MX = medium-scale cross-bedding, and R = total number of readings. A  $30^{\circ}$ -sliding average was used in preparation of the diagram. Grain orientation taken from Figure 21.

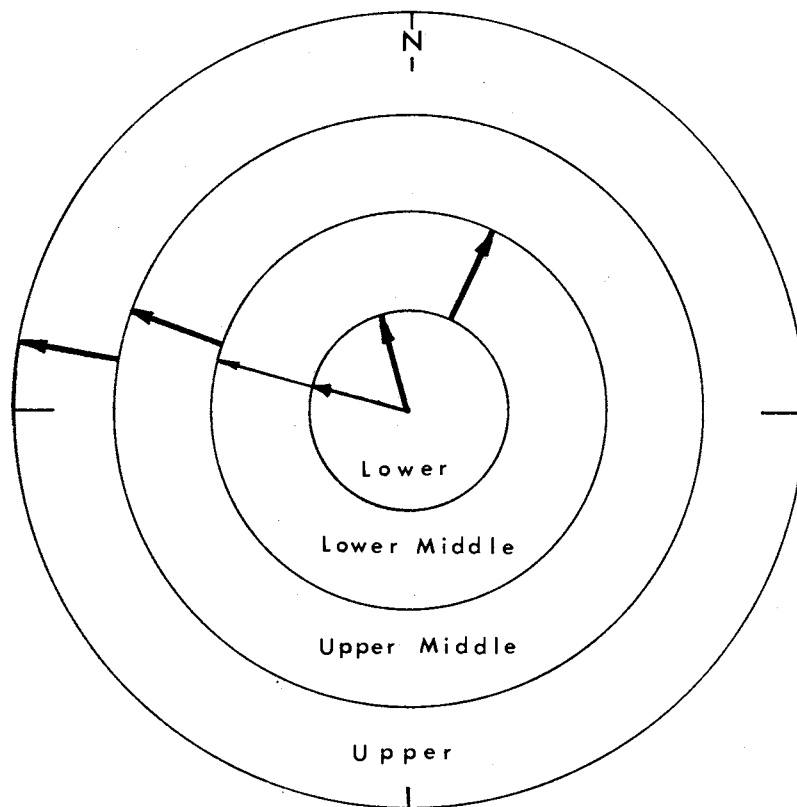


Figure 25. Diagram illustrating an overall westerly change in paleocurrent direction with time. Large arrows denote primary grain orientation trends and small arrows denote secondary trends.

## CHAPTER VI

### GRAIN ORIENTATION IN A BRAIDED-MEANDERING

#### STREAM: CIMARRON RIVER

The Cimarron River flows from northeastern New Mexico, eastward, to its confluence with the Arkansas River in Keystone Reservoir, just west of Tulsa, Oklahoma. It is characterized along the eastern part of its course by features of both a braided and meandering stream. In this study, grain orientation measured both in the field and laboratory is compared to other directional features in deposits of the river.

#### Geologic Setting

In the study area at Perkins, Oklahoma, the Cimarron River deposits overlie Permian redbeds. Grain orientation was examined on a sand bar where lateral accretion, from south to north, forms an arcuate curve, or meander. The sand contains horizontal bedding, as well as medium- and small-scale cross-bedding. The sediments composing the bar are generally fine- to medium-grained, with occasional pebbles and clay galls. Clay drapes separate some of the individual depositional events and scattered concentrations of heavy minerals occur principally in horizontal strata.

## Grain Orientation

### In Situ Measurements

Field study was made in August, 1972, in collaboration with R. L. Noble (1973) who is presently examining the river deposits of the Cimarron at Perkins. In the area of approximately 2 square mi., 6 trenches were dug by a tractor-mounted backhoe down to the water table, at an average depth of 6 to 8 ft. with the remaining part of the area sampled according to a grid pattern. For each location, sedimentary structures were noted and a current direction was ascertained. These directions were measured in 27 medium-scale cross-beds, 12 small-scale cross-beds, and 5 horizontal beds. Current directions in horizontal beds were measured by parting lineation. Grain orientation was then measured in the field with the COBRA instrument, utilizing an in situ probe. Overall, the grain orientation shows good correlation with the other current indicators and with the trends of the sand body in the valley (Figures 26-28). The dominant trend of grain orientation is  $N85^{\circ}E$ , which varies  $30^{\circ}$  from the average direction of medium-scale cross-bedding,  $20^{\circ}$  from the average direction of small-scale cross-bedding, and  $25^{\circ}$  from the average direction of parting lineation.

### Laboratory Measurements

In addition to the in situ measurements in the field, 4 undisturbed samples were collected, impregnated with an epoxy cement, drilled, and measured by standard laboratory procedures. The primary purpose was to compare laboratory measurements to the in situ



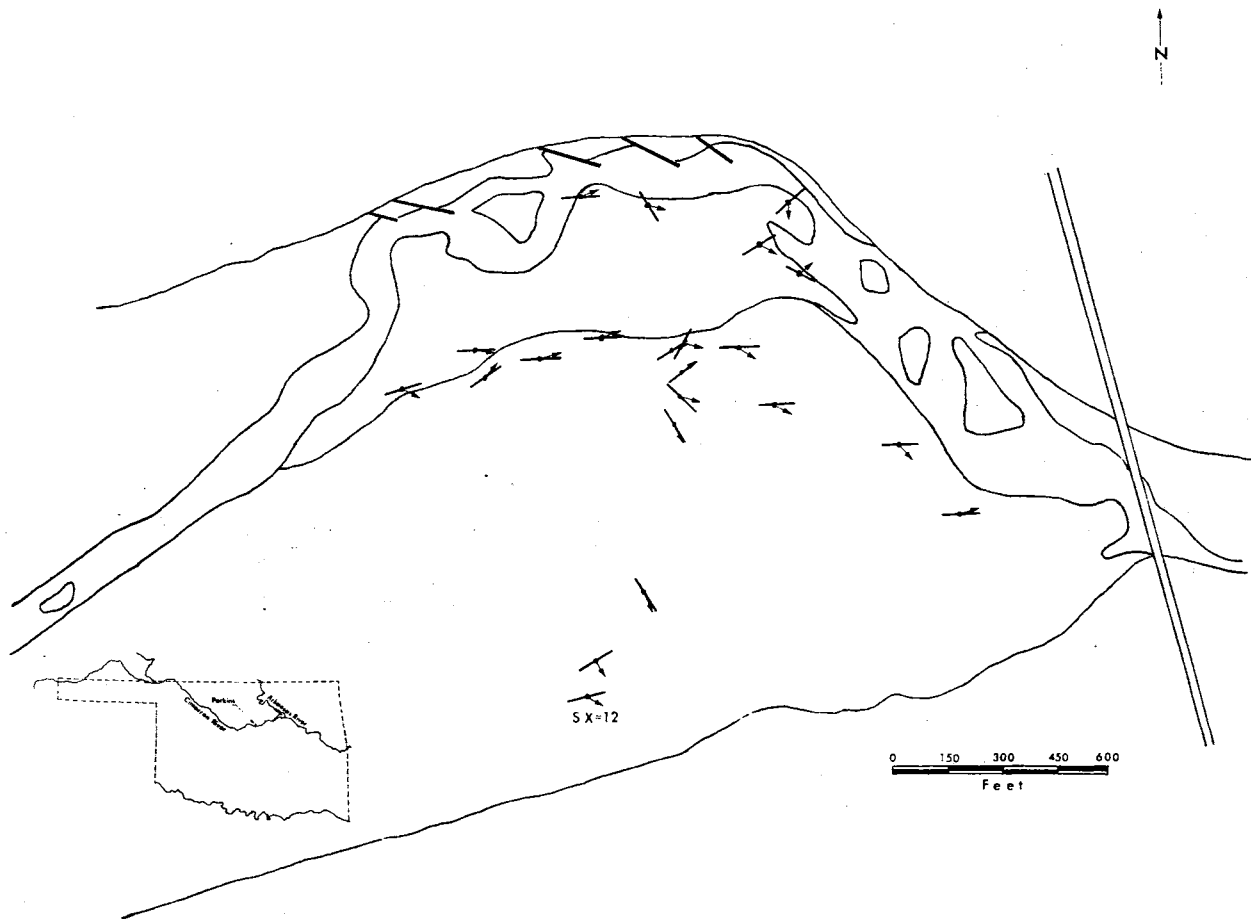


Figure 26. Map of study area, showing current directions for medium-scale cross-bedding (with arrow) and grain orientation. SX = 12 at southernmost locality refers to 12 small-scale cross-bed measurements.

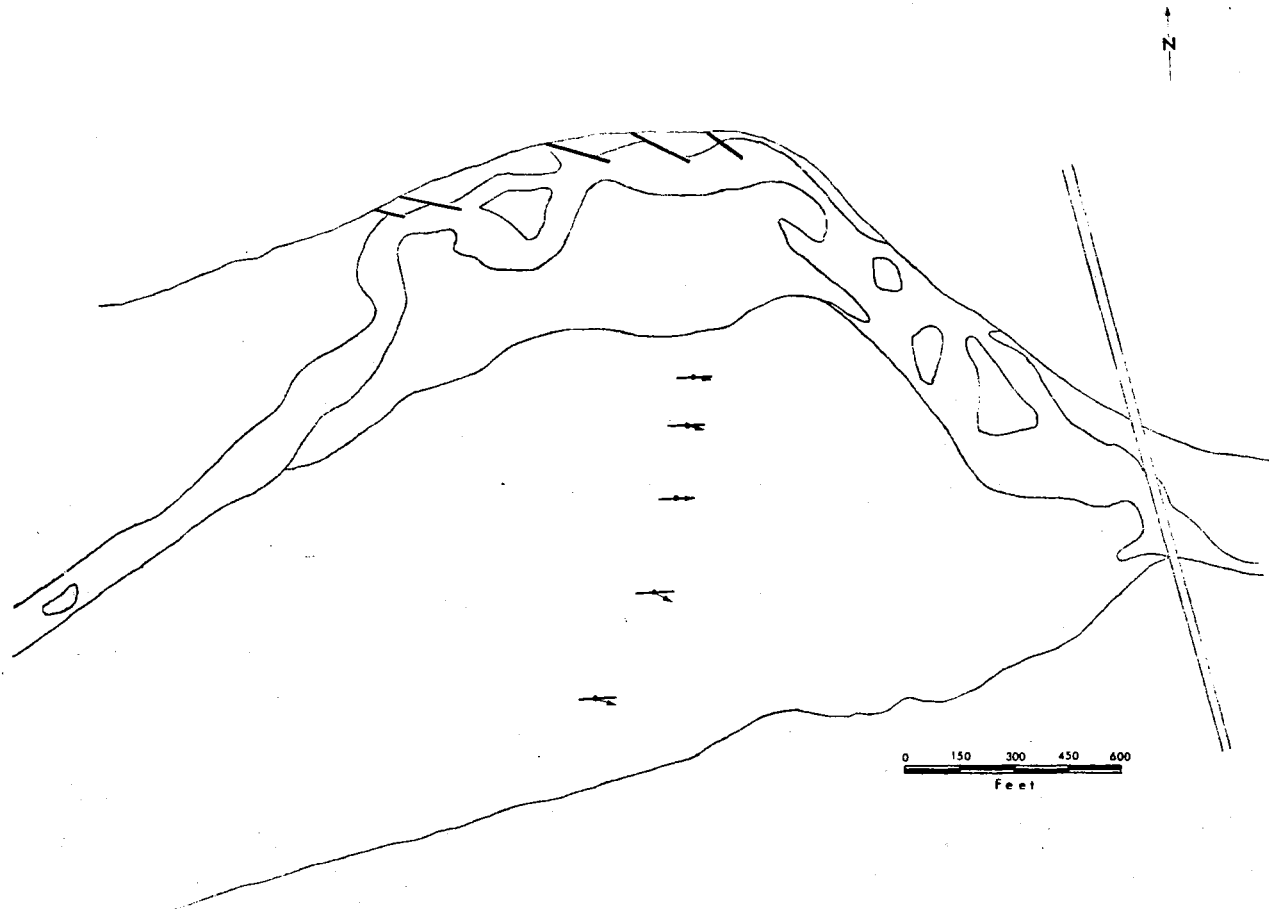


Figure 27. Map of study area, showing current trends from parting lineation in horizontally bedded sand (with arrows) and grain orientation.

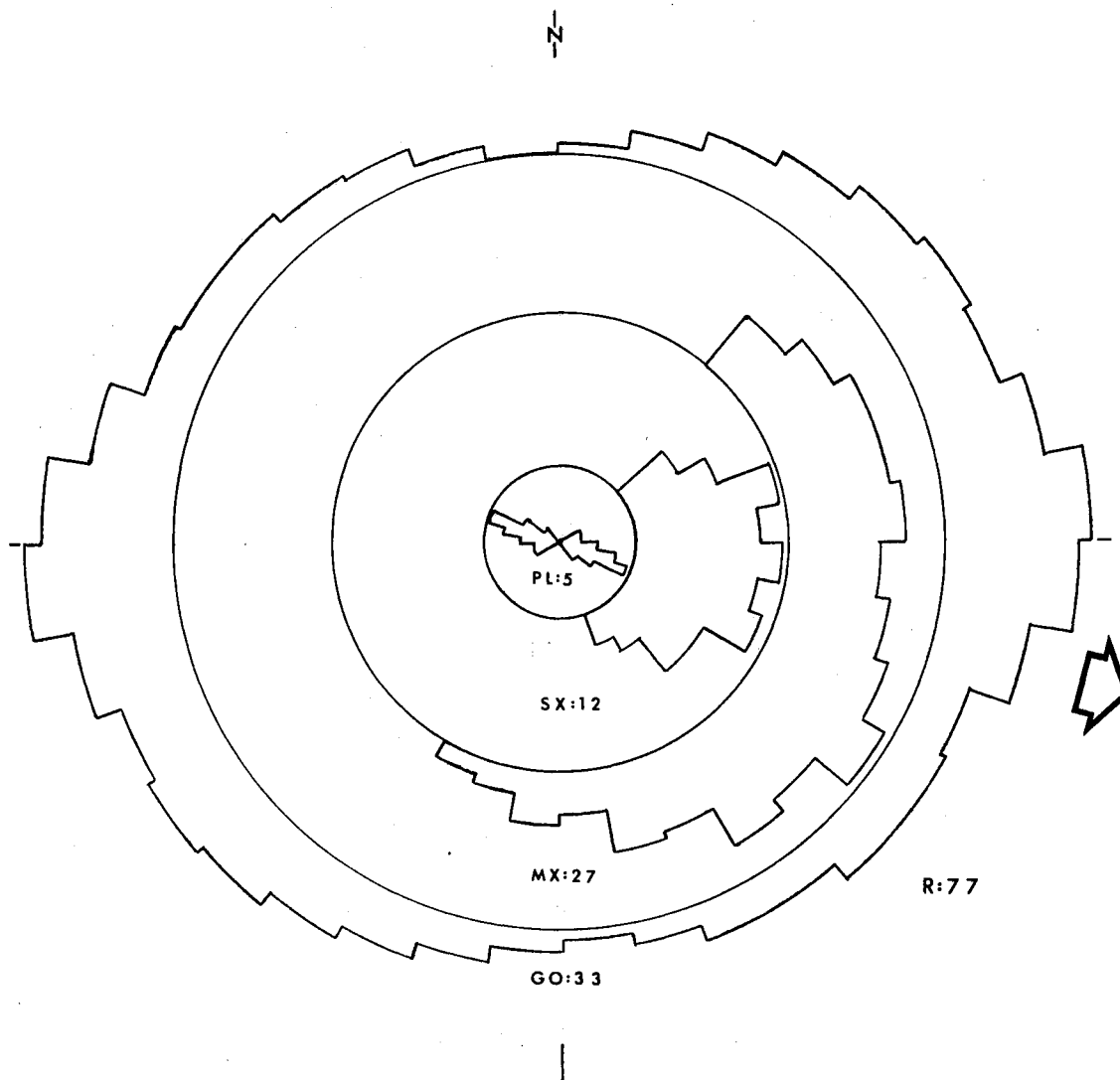


Figure 28. Directional features in Cimarron River sand deposits, with an average direction of  $S75^{\circ}E$ . Key to abbreviations is given in Figure 24. A  $30^{\circ}$ -sliding average was used in preparation of the diagram.

measurements. The results of that study show good correlation (Table VIII; Figures 29 and 30). In situ measurements compare more closely to the current indicators than do the laboratory measurements. The divergence between in situ and laboratory measurements is less in horizontal beds than in medium-scale cross-beds. Overall, the results of both grain orientation methods and current indicators reflect the expected strong eastward current direction.

TABLE VIII

Comparison of Grain Orientation Measurements to Other Current Indicators

Bedding Feature	C <sup>1</sup>	I <sup>2</sup>	L <sup>3</sup>	C vs. I	C vs. L	I vs. L	Quality <sup>4</sup> of L
Horizontal Beds	S89°E	S90°E	N70°E	1°	21°	20°	F,P
Medium- Scale Cross-Beds	N75°E	N60°E	S82°E	15°	23°	38°	G,P

<sup>1</sup> Average current direction from visual current indicators.

<sup>2</sup> Average in situ grain orientation.

<sup>3</sup> Average laboratory grain orientation.

<sup>4</sup> See Appendix E for rating of quality of results. G = Good, F = Fair, P = Poor.

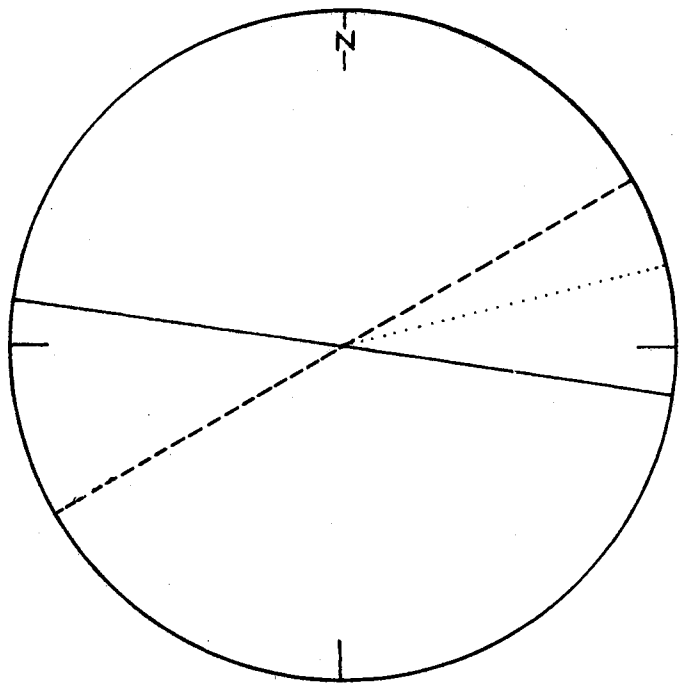


Figure 29. Diagram comparing laboratory (solid line) and in situ (dashed line) measurements of grain orientation in medium-scale cross-bedding. Dotted line is current direction measured by medium-scale cross-bedding.

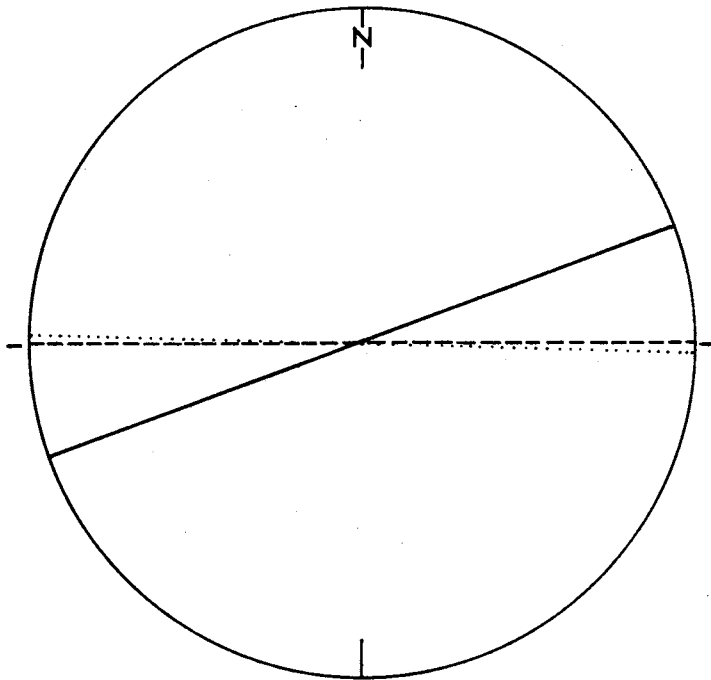


Figure 30. Diagram comparing laboratory (solid line) and in situ (dashed line) measurements of grain orientation in horizontal beds. Dotted line is current direction measured by parting lamination.

## CHAPTER VII

### SUMMARY

The principal conclusions of this study are as follows:

1. The Recent Galveston Island barrier sand shows grain orientation almost normal to the trend and imbrication dipping shoreward at  $4^{\circ}$ ; the latter indicates the dominant influence of backwash, although some evidence suggests some deposition by wash.

2. The lowermost unit of the Cretaceous Eagle Sandstone represents a barrier-bar deposit. Grain orientation is perpendicular to the trend, and imbrication dipping shoreward at  $7^{\circ}$  indicates that backwash was the dominant depositing current. Variation in plug measurements and thin-section analysis suggest some influence from wash.

3. The Ordovician Harding Sandstone was deposited in a shallow marine environment. Preferred grain orientation is  $83^{\circ}$  from the sandstone trend interpreted from a lithofacies map. The imbrication angle is  $8^{\circ}$  seaward, a relationship suggesting deposition from wave-related currents moving shoreward.

4. The Ordovician Burgen Sandstone is a nearshore or shoreface deposit. The grain orientation is at a high angle to the western flank of the Ozark uplift, and probably to the shoreline along the uplift. An eastward dip of  $18^{\circ}$  suggests backwash as the dominant depositional agent.

5. The Upper Cretaceous Trinidad Sandstone represents a nearshore shallow marine environment. Grain orientation is approximately perpendicular to trend, and imbrication is dipping shoreward at  $10^{\circ}$ . Backwash is suggested as the dominant sand-depositing agent.

6. In the Pennsylvanian Vamoosa Formation, grain orientation correlates very well with other paleocurrent indicators. A westerly change in average grain orientation with time may possibly reflect changes in source areas.

7. The Cimarron River data show excellent correlation between grain orientation and other paleocurrent indicators associated with the sediments. Both of these types of data show good correlation with the trend of the sand body. This study proves that the COBRA, with its in situ probe, is well adapted to field use.

8. Accuracy and precision increase as the number of analyses increase, especially for deltaic sandstones.

9. Grain orientation studies in massive beds which show gross horizontal stratification should be coupled with radiography in order to avoid analysis of grain orientation in bioturbated beds.



#### REFERENCES CITED

- Arbogast, J. L., 1960, Method and apparatus for determining directional dielectric anisotropy in solids: U. S. Patent 2,963,642.
- Asquith, D. O., 1970, Depositional topography and major marine environments, Late Cretaceous, Wyoming: Am. Assoc. Petroleum Geologists Bull., v. 54, p. 1184-1224.
- Bernard, H. A., R. J. LeBlanc, and C. F. Major, 1962, Recent and Pleistocene geology of southeast Texas, in Geology of Gulf Coast and central Texas and guidebook of excursions: Houston Geol. Society (for Geol. Soc. America, 1962 meeting), p. 175-224.
- Bonham, L. C., 1957, Structural petrology of the Pico Anticline, Los Angeles County, California: Jour. Sed. Petrology, v. 32, p. 251-264.
- Cram, I. H., 1930, Cherokee and Adair Counties: Oklahoma Geol. Survey Bull. 40, p. 531-586.
- Curray, J. R., 1956, Dimensional grain orientation studies of Recent coastal sands: Am. Assoc. Petroleum Geologists Bull., v. 40, p. 2440-2456.
- Dapples, E. C., and J. F. Rominger, 1945, Orientation analysis of fine-grained clastic sediments: a report of progress: Jour. Geology, v. 53, p. 246-261.
- DeFord, R. K., 1929, Surface structure, Florence oil field, Fremont County, Colorado, in Structure of typical American oil fields: Am. Assoc. Petroleum Geologists, p. 75-92.
- Dodge, C. F., ed., 1968, Stratigraphy of the Woodbine Formation, Tarrant County, Texas: 2d Ann. Mtg. South-Central Sec. Geol. Soc. America, Field Trip Guidebook, 76 p.
- Foster, N. H., 1972, Ordovician System, in Geologic atlas of the Rocky Mountain region, U.S.A.: Rocky Mtn. Assoc. Geologists, p. 76-85.
- Gill, J. R., and W. A. Cobban, 1969, Paleogeographic maps, Western Interior: U.S. Geol. Survey Open File Report, 6 sheets.
- Gore, C. E., 1952, Geology of a part of the drainage basins on Spavinaw, Salina, and Spring Creeks, northeastern Oklahoma: Tulsa Geol. Soc. Digest, v. 20, p. 144-179.

- Greig, P. B., 1959, Geology of Pawnee County, Oklahoma: Oklahoma Geol. Survey Bull. 83, 188 p.
- Hand, B. M., 1961, Grain orientation in turbidites: *Compass*, v. 38, p. 133-144.
- Helmbold, R., 1961, Contribution to the petrology of the Tanner Graywacke: *Geol. Soc. America Bull.*, v. 49, p. 301-314.
- Hsu, J. K., 1960, Texture and mineralogy of the Recent sands of the Gulf Coast: *Jour. Sed. Petrology*, v. 30, p. 380-403.
- Huffman, G. G., 1958, Geology of the flanks of the Ozark uplift, northeastern Oklahoma: *Okla. Geol. Survey Bull.* 77, 281 p.
- \_\_\_\_\_, J. M. Langston, and J. M. Hancock, 1966, Geology of northern Adair County, Oklahoma: *Okla. Geol. Survey Circ.* 68, 50 p.
- Johnson, R. B., and G. H. Wood, Jr., 1956, Stratigraphy of Upper Cretaceous and Tertiary rocks of Raton basin, Colorado and New Mexico: *Am. Assoc. Petroleum Geologists Bull.*, v. 40, p. 289-352.
- Levorsen, A. I., 1930, Geology of Seminole County: *Oklahoma Geol. Survey Bull.* 40, v. 3, p. 289-352.
- Martinez, J. D., 1958, Photometer method for studying quartz grain orientation: *Am. Assoc. Petroleum Geologists Bull.*, v. 42, p. 588-608.
- Martinni, I. P., 1971, A test of validity of quartz grain orientation as a paleocurrent and paleoenvironmental indicator: *Jour. Sed. Petrology*, v. 41, p. 60-68.
- Mast, R. F., and P. E. Potter, 1963, Sedimentary structures, sand shape fabrics, and permeability. II.: *Jour. Geology*, v. 71, p. 548-565.
- Matuszczak, R. A., 1969, Trinidad Sandstone, interpreted, evaluated, in Raton basin, Colorado-New Mexico: *The Mountain Geologist*, v. 6, p. 119-124.
- Matalucci, R. V., J. W. Shelton, and M. Abdel-Hady, 1969, Grain orientation in Vicksburg loess: *Jour. Sed. Petrology*, v. 39, p. 969-979.
- McGookey, D. P., 1972, Cretaceous System, in *Geologic atlas of the Rocky Mountain region, U.S.A.*: *Rocky Mtn. Assoc. Geologists*, p. 190-228.
- Nanz, R. H., 1955, Grain orientation in beach sands: a possible means for predicting reservoir trend (abs.): *Program Soc. Econ. Paleon, Mineralogists 29th Ann. Meeting*, New York.

- \_\_\_\_\_, 1960, Exploration of earth formations associated with petroleum deposits: U.S. Patent 2,963,641.
- Noble, R. L., 1973, (in press) Depositional and directional features of a braided-meandering stream: M. S. Thesis, Oklahoma State Univ.
- Oakes, M. C., 1959, Geology of Creek County, Oklahoma: Oklahoma Geol. Survey Bull. 81, 134 p.
- Orr, W. R., 1964, Method for determining directional inductive anisotropy of materials by measuring Q factor: U.S. Patent 3,151,292.
- Pettijohn, F. J., 1962, Paleocurrents and paleogeography: Am. Assoc. Petroleum Geologists Bull., v. 46, p. 1468-1493.
- Pierson, A. L., 1959, A photomultiplier for studying quartz grain orientation: Jour. Sed. Petrology, v. 29, p. 98-103.
- Pincus, H. J., and M. B. Dobrin, 1966, Geological applications of optical data processing: Jour. Geophysical Res., v. 71, p. 4861-4869.
- Rees, A. I., 1971, The magnetic fabric of a sedimentary rock deposited on a slope: Jour. Sed. Petrology, v. 41, p. 307-309.
- Ries, E. R., 1954, Geology and mineral resources of Okfuskee County, Oklahoma: Oklahoma Geol. Survey Bull. 71, 120 p.
- Rodriguez, A. R. and S. J. Pirson, 1968, The continuous dipmeter as a tool for studies in directional sedimentation and tectonics: Soc. Prof. Well Log Analysts 9th Ann. Logging Symposium, p. G1-G25.
- Rowland, R. A., 1940, Petrofabric determination of quartz grain orientation in sediments (abs.): Geol. Soc. America Bull., v. 51, p. 1941-1942.
- Rusnak, G. A., 1957, The orientation of sand grains under conditions of "unidirectional" fluid flow: Jour. Geology, v. 65, p. 384-409.
- Schwarzacher, W., 1951, Grain orientation in sands and sandstones: Jour. Sed. Petrology, v. 21, p. 162-172.
- Shelton, J. W., 1965, Trend and genesis of lowermost sandstone unit of Eagle Sandstone at Billings, Montana: Am. Assoc. Petroleum Geologists Bull., v. 49, p. 1385-1397.
- \_\_\_\_\_, and D. E. Mack, 1970, Grain orientation in determination of paleocurrents and sandstone trends: Am. Assoc. Petroleum Geologists Bull., v. 54, p. 1108-1119.

- Spotts, J. H., 1964, Grain orientation and imbrication in Miocene turbidity current sandstones, California: Jour. Sed. Petrology, v. 34, p. 229-253.
- Stark, J. M., 1961, Geology of northeastern Cherokee County, Oklahoma: Oklahoma Geol. Survey Circ. 57, 62 p.
- Sweet, W. C., 1954, Harding and Fremont Formations, Colorado: Am. Assoc. Petroleum Geologists Bull., v. 38, p. 284-305.
- Tanner, W. F., 1956, Geology of Seminole County, Oklahoma: Oklahoma Geol. Survey Bull. 74, 175 p.
- Terrell, D. M., 1972, Trend and genesis of the Pennsylvanian Elgin Sandstone in the western part of northeastern Oklahoma: Unpub. M.S. Thesis, Oklahoma State Univ., 79 p.
- Weimer, R. J., 1960, Upper Cretaceous stratigraphy, Rocky Mountain area: Am. Assoc. Petroleum Geologists Bull., v. 44, p. 1-20.
- Winkelmolen, A. M., 1972, Dielectric anisotropy and grain orientation: Am. Assoc. Petroleum Geologists Bull., v. 56, p. 2150-2159.
- Zimmerle, W., and L. C. Bonham, 1962, Rapid methods for dimensional grain orientation measurements: Jour. Sed. Petrology, v. 32, p. 751-763.

APPENDIX A

COBRA MEASUREMENT

1. The core (plug) should be smooth and the two ends parallel with each other and perpendicular to the cylindrical axis. Ordinary tap water should be used to saturate the cores and fill the cell.
2. Cores should be saturated by vacuum impregnation. The cores to be water-saturated are placed in a cell jar; the vacuum valve is closed; and water is admitted from a vessel above. Sufficient water should be admitted to cover the cores completely. Allow the cores to remain in the water for 1 to 2 days so that equilibrium is reached.
3. Fill the cell with the water in which the cores reside. Fill the cell in such a way that no air bubbles are trapped.
4. Turn the GAIN control from OFF to BATT in order to check the voltage. The needle of the meter should read near the dot on the left of the scale. Rotate the VERNIER control fully counterclockwise and advance the GAIN to position 1. The bridge is now in operation, and the needle should show some deflection prior to the following balancing procedures.
5. Obtain a resistance balance by adjusting the RES control. It may also be necessary to adjust the resistance range control marked RANGE K. A resistance balance is indicated when the needle points to the center dot on the meter face.
6. Now push the switch marked PHASE fully to the right (to  $C 90^\circ$ ), and holding it in this position, adjust the CAP and E CAP controls for a capacitance bridge balance. Allow the phase switch to return to its normal position and recheck the resistance balance. Advance the VERNIER control fully clockwise and repeat the above balancing procedure.

7. Advance the GAIN control to position 2 and rotate the VERNIER fully counterclockwise. Check the resistance and capacitance bridge balances. Advance the VERNIER control fully clockwise and readjust the bridge balance.

8. Advance the GAIN control to position 3 and leave the VERNIER control fully clockwise. If necessary, readjust the RES and CAP controls to balance.

9. Rotate the glass shaft until the index lines on the viewer are aligned with either  $90^\circ$  or  $270^\circ$  on the calibrated drum. Place a water-saturated core in the core holder so that the reference line on the core is aligned with the two index lines on the cell. Make sure the water level in the cell is above the top of the core and that the core rotates concentrically with the glass shaft.

10. Rotate the core through a complete revolution to test for meter deflection.

11. The GAIN and VERNIER controls should be adjusted so that the needle remains on scale as the core is rotated. The PHASE switch should always be in its normal, or  $R^\circ$ , position when a core is being measured. Position 3 of the GAIN control is used for most measurements.

12. Use the glass shaft to rotate the core until the maximum deflection of the needle to the left is obtained. (Left refers to the operator's left as he faces the instrument.) Carefully oscillate the core back and forth to determine the exact position of maximum conductivity on the drum opposite the index mark on the viewer. There should be two angular positions of maximum conductivity per revolution, and these positions should be  $180^\circ$  apart.

13. The angular positions of maximum conductivity are measured counterclockwise from the reference mark on the core.

14. Rotate the GAIN control back to the BATT position and remove the core from the core holder.

15. Place a new core in the core holder and follow the same procedure as before.



APPENDIX B

IN SITU MEASUREMENT

Measurements obtained in the field differ from the laboratory method basically in that grain orientation is measured externally rather than internally, with respect to the instrument. An adapting probe with 12 small plates, arranged in 6 circuits, is inserted into the sediments rather than the impregnated sediment core being placed into the core holder. A switch box, making alternating contact with the different circuits, is placed in the circuit between the instrument and the probe. The following steps are recommended for field use.

1. Disconnect and remove wire leads from the core holder and remove it because it is not needed in the field. The rotating shaft is very fragile and should be handled with care.

2. Attach the leads to the posts of the switch box and check for continuity by inserting the probe into a beaker of water. If a deflection on the meter occurs, with the GAIN in position 1, the instrument is now field-worthy.

3. In the field, prepare a measurement site by scraping the sand to form a horizontal surface. Then carefully push a large plastic sleeve, with a tapered end, into the sand. Recommended dimensions for the pipe are 3 to 4 in. in diameter and 3 to 4 in. long.

4. A plastic plate is then pushed into the sand underneath the sleeve. This plate prevents the water from flowing out of the sample area too rapidly.

5. Place a paper towel on the sand. Pour water on this surface and allow it to percolate down through the sand and saturate it completely.

6. After aligning the probe with geographical coordinates for reference, push it into the sample until the base of the probe is about

$\frac{1}{4}$  in. above the top of the sand. The plates then extend approximately  $1\frac{1}{4}$  in. into the sample.

7. Carefully cover the area around the perimeter of the plates and within the walls of the plastic sleeve with paper towels. This procedure aids in avoiding disturbance of the grains as water is added.

8. Add water until it stands inside the plastic sleeve yet does not touch the base of the probe. In order that complete saturation of the sample is accomplished, the water level should coincide with the top surface of the sand.

9. Advance the GAIN control to position 1 on the instrument and balance the bridge as described in steps 5 to 8 in Appendix A. Water flowing through the sand may cause fluctuation and difficulty in balancing the bridge. After it is balanced, rotate the knob on the switch until maximum deflection to the left is obtained. Make a duplicate measurement for accuracy.

10. Saturate the sand again with water and repeat step 9. If consistent results are obtained, the measurement is recorded. Quality of measurement is made on the basis of the degree of deflection and consistency of results.

Coordination and practice is necessary for proficiency in making measurements. It is recommended that the measurements be taken by a team of 2 or 3 workers so that equipment can be handled efficiently.

APPENDIX C

IMPREGNATION TECHNIQUES

1. A thin-walled sleeve is recommended for obtaining samples of unconsolidated sand. A can or leucite tube, 3 to 4 in. in diameter and 4 to 5 in. long, is preferred.

2. Push the sleeve, with properly chosen reference mark, into the sand until it is full. Place paper towels at each end for packing in a sealed plastic wrap.

3. In the laboratory, unwrap one end and remove  $\frac{1}{2}$  in. of sand. If the sand is dry, proceed to step 4. If sample is wet, saturate it with isopropyl alcohol and allow it to dry.

4. Mix solution of acetone and small pieces of plastic until consistency is uniform and add fine silt or clay to form a highly viscous fluid. Pour the fluid into the top of the sleeve. Cure for 24 hours at  $105^{\circ}\text{C}$ . so that plastic plug forms a water-tight seal.

5. Unwrap the other end of the sample and remove  $\frac{1}{2}$  in. of sand.

6. Mix solution of the epoxy cement (eposand A, B, and C) in the following volumetric ratios: 50/50/7, respectively. Carefully saturate sample with solution.

7. Cure eposand for 24 hours at  $105^{\circ}\text{C}$ .

8. Repeat step 6.

9. Repeat step 7.

10. Repeat step 6.

11. Cure eposand for 48 hours at  $105^{\circ}\text{C}$ .

12. To remove sample from can, cut a shallow groove with a diamond saw along the seam. Remove sleeve and allow sample to cool before drilling plugs. Where leucite sleeve is used, sample may remain in sleeve during drilling of plugs.

13. Drill plugs to a minimum length of  $1\frac{1}{4}$  in.

14. Face plugs so that ends are perpendicular to axis and length is  $7/8$  in.

15. Place plugs in beaker of isopropyl alcohol for 24 hours at room temperature.

16. Drain alcohol and repeat step 15.

17. Place plugs in a vacuum chamber that has a connecting water flask. Pull a vacuum for an hour and then release enough water to cover plugs. Remove plugs and place in a covered jar containing the saturating water. Plugs are now ready for analysis.

APPENDIX D

COMPUTER PROGRAM: CHAYES' MINIMUM

VARIANCE FABRIC MEAN

```

1  $JOB *****kp=026 BURMAN, RICHARD
2  DIMENSION Y(20),X(20),SY(20),AX(20),Z(20),DIFF(20),AK(20),VI(20)
3  READ 1,IPAR
4  11 FORMAT(I4<
5  DO 12 I = 1,IPAR,1
6  READ 14, X(1),X(2),X(3),X(4),X(5),X(6),X(7),X(8),X(9),SPEC
7  READ 14,X(10),X(11),X(12),X(13),X(14),X(15),X(16),X(17),X(18)
8  14 FORMAT (F4.0,F4.0,F4.0,F4.0,F4.0,F4.0,F4.0,F4.0,F4.0,F4.0,28X,F8.1<
9  READ 14,Y(1),Y(2),Y(3),Y(4),Y(5),Y(6),Y(7),Y(8),Y(9)
10 READ 14,Y(10),Y(11),Y(12),Y(13),Y(14),Y(15),Y(16),Y(17),Y(18)
11 PRINT 101
12 101 FORMAT (//1H1,16H SPECIMEN NUMBER<
13 PRINT 103, SPEC
14 103 FORMAT (36X,28X,F8.1<
15 SF = 0.0
16 SY 18 = 0.0
17 DO 15 I = 1,18,1
18 15 SY 18 = SY 18 + Y(I)
19 SYY = 0.0
20 DO, 5 I = 1,18,1
21 CUM = X(I)*Y(I)
22 SF = SF + CUM
23 SYY = SYY + Y(I)
24 SY(I) = SYY/SY 18
25 5 AX(I) = SF/SYY
26 GO TO 31
27 31 AVEX = SF / SY 18
28 SZ = 0.0
29 I = 1
30 DO 7 I = 1,18,1
31 Z(I) = X(I)*X(I)*Y(I)
32 SZ = SZ + Z(I)
33 7 CONTINUE
34 S2MOM = SZ/SY 18
35 VAR = (S2MOM - (AVEX**2))
36 STDV = VAR**0.5
37 SNED = 2700.0/ VAR
38 PRINT 13
39 13 FORMAT (//5X,7H AVEX,4X,10H VARIANCE,4X,8H STDV<
40 PRINT 27, AVEX,VAR,STDV
41 27 FORMAT (5X,F7.2,4X,F10.3,4X,F8.3<
42 PRINT 28
43 28 FORMAT (//5X,8H SNED,4X,7H SY 18<
44 PRINT 29,SNED,SY 18
45 29 FORMAT (5X,F8.4,4X,F7.1<
46 PRINT 8
47 8 FORMAT (///10X,3HLCL,4X,4HFREQ,6X,2HVI<
48 DO 90 I=1,18,1
49 DIFF(I) = AX(I) - AX(18)
50 AK(I) = 90.0*(1.0-SY(I))
51 VI(I) = (DIFF(I) + AK(I))*(SY(I))
52 90 PRINT 9,X(I),Y(I),VI(I)
53 9 FORMAT (10X,F4.0,3X,F4.0,3X,F7.4<
54 VIMX = VI(1)
55 KK = 1
56 DO 20 K = 2,18,1
57 IF (VIMX - VI(K)) 21,20,20
58 21 VIMX = VI(K)
59 KK = K
60 CONTINUE

```



```

60      PRINT 16
61      16 FORMAT (//5X,8H      VIMX,5X,4H  KK,5X,5HX(KK)<
62      PRINT 10,VIMX,KK,X(KK)
63      10 FORMAT (5X,F8.4,5X,I4,5X,F5.0<
64      XX = X(KK)
65      DO 40 I = 1,18,1
66      X(I) = X(I) - XX
67      IF (XX) 30,105,32
68      30 IF (X(I) - 90.0) 40,40,41
69      41 X(I) = X(I) - 180.0
70      GO TO 40
71      105 PRINT 107
72      107 FORMAT (11H VAR IS MIN<
73      GO TO 12
74      32 IF (X(I) + 85.0) 50,50,40
75      50 X(I) = X(I) + 180.0
76      40 CONTINUE
77      SF = 0.0
78      SY 18 = 0.0
79      DO 18 I = 1,18,1
80      18 SY 18 = SY 18 + Y(I)
81      SYY = 0.0
82      DO 1 I = 1,18,1
83      CUM = X(I)*Y(I)
84      SF = SF + CUM
85      SYY = SYY + Y(I)
86      SY(I) = SYY/SY 18
87      1 AX(I) = SF/SYY
88      GO TO 33
89      33 AVEX = SF/ SY 18
90      SZ = 0.0
91      I = 1
92      DO 3 I = 1,18,1
93      Z(I) = X(I)*X(I)*Y(I)
94      SZ = SZ + Z(I)
95      3 CONTINUE
96      S2MQM = SZ/SY 18
97      VAR = (S2MQM - (AVEX**2))
98      STDV = VAR**0.5
99      SNED = 2700.0/ VAR
100     PRINT 80
101     80 FORMAT (//5X,7H  AVEX,4X, 9H VARIANCE,4X,8H  STDV<
102     PRINT 81, AVEX,VAR,STDV
103     81 FORMAT (5X,F7.2,4X,F10.3,4X,F8.3<
104     PRINT 82
105     82 FORMAT (//5X,8H  SNED,4X,7H  SY 18<
106     PRINT 83,SNED,SY 18
107     83 FORMAT (5X,F8.4,4X,F7.1<
108     12 CONTINUE
109     GO TO 140
110     140 STOP
111     END

```

\$ENTRY

SPECIMEN NUMBER: 69 B

AVEX	VARIANCE	STDV
14.62	3644.892	60.373

SNED	SY 18
0.7408	509.0

LCI	FREQ	VI
-80.	54.	-1.5028
-70.	28.	-2.5295
-60.	39.	-4.1010
-50.	17.	-4.7828
-40.	9.	-5.0482
-30.	14.	-5.2978
-20.	13.	-5.3962
-10.	15.	-5.3609
0.	20.	-5.1640
10.	20.	-4.8521
20.	18.	-4.4554
30.	18.	-3.9302
40.	19.	-3.2467
50.	24.	-2.2703
60.	48.	-0.5751
70.	52.	0.4766
80.	57.	0.5910
90.	44.	0.0000

VIMX	KK	X(KK)
0.5910	17	80.

AVEX	VARIANCE	STDV
1.45	1714.979	41.412

SNED	SY 18
1.5744	509.0

X(KK) = Lower Class Limit = 80 = N80°E

AVEX = Mean (overall) = 1.45° (additive)

Bearing = N81°E

North Azimuth = 81°

STDV = Standard Deviation = 41°

SNED = Variance Ratio, F = 1.57

APPENDIX E

RATING OF QUALITY OF RESULTS

RATING OF QUALITY OF RESULTS<sup>1</sup>

No. Measurements	Range					
	20°	30°	40°	50°	60°	90°
2	G	G	F	F	P	
3	E	G	G	F	F	
4	E	E	G	G	F	P
5	E	E	E	G	F	P
6	E	E	E	G	G	F

<sup>1</sup>From Shelton and Mack (1970)

VITA

Howard Richard Burman, Jr.

Candidate for the Degree of

Master of Science

Thesis: GRAIN ORIENTATION, PALEOCURRENTS, AND RESERVOIR TRENDS

Major Field: Geology

Biographical:

Personal Data: Born in Borger, Texas, August 28, 1949, the son of Mr. and Mrs. Howard R. Burman, Sr.

Education: Graduated from College High School, Bartlesville, Oklahoma, in May, 1967; completed the requirements for a Bachelor of Science degree in geology from Oklahoma State University, Stillwater, Oklahoma, in January, 1971; completed requirements for the Master of Science degree at Oklahoma State University in May, 1973, with a major in geology.

Professional Experience: Mud Logging Engineer, Core Laboratories, Inc., Aug.-Dec., 1971; Crew Chief-Mud Logging Unit, Core Laboratories, Inc., summer, 1972; Graduate Assistant, Department of Geology, Oklahoma State University, 1973. Junior Member of the American Association of Petroleum Geologists.